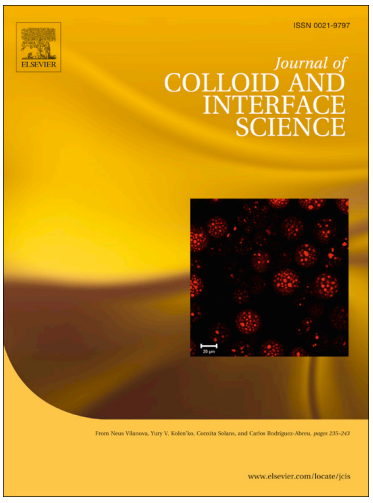

Advances in colloidal manipulation and transport via hydrodynamic interactions

F. Martínez-Pedrero, P. Tierno

PII: S0021-9797(18)30218-2
DOI: https://doi.org/10.1016/j.jcis.2018.02.062
Reference: YJCIS 23334

To appear in: *Journal of Colloid and Interface Science*

Received Date: 18 December 2017
Revised Date: 19 February 2018
Accepted Date: 19 February 2018

Please cite this article as: F. Martínez-Pedrero, P. Tierno, Advances in colloidal manipulation and transport via hydrodynamic interactions, *Journal of Colloid and Interface Science* (2018), doi: https://doi.org/10.1016/j.jcis.2018.02.062

Advances in colloidal manipulation and transport via hydrodynamic interactions

F. Martínez-Pedrero[1,], P. Tierno[2,3,4].*

[1]Departamento de Química-Física I, Universidad Complutense de Madrid, Avda. Complutense s/n, Madrid, 28040, Spain.

[2]Departament de Física de la Matèria Condensada, Universitat de Barcelona, E-08028, Barcelona, Spain

[3]Universitat de Barcelona Institute of ComplexSystems(UBICS), Universitat de Barcelona, E-08028, Barcelona, Spain.

[4]Institut de Nanociència i Nanotecnologia, IN^{2}UB, Universitat de Barcelona, E-08028, Barcelona, Spain.

* fernandm@ucm.es

KEYWORDS: Colloids, Propulsion at low Reynolds number, Hydrodynamic interactions, Bound states, Synchronization.

ABSTRACT. In this review article, we highlight many recent advances in the field of micromanipulation of colloidal particles using hydrodynamic interactions (HIs), namely solvent mediated long-range interactions. At the micrsocale, the hydrodynamic laws are time reversible and the flow becomes laminar, features that allow precise manipulation and control of colloidal matter. We focus on different strategies where externally operated microstructures generate local flow fields that induce the advection and motion of the surrounding components. In addition, we review cases where the induced flow gives rise to hydrodynamic bound states that may synchronize during the process, a phenomenon essential in different systems such as those that exhibit self-assembly and swarming.

1. Introduction

In the past few years, there have been significant advances on the control of the matter at the microscale [1-6]. When microparticles are dispersed in a liquid, they are subjected to interactions mediated by the suspending medium, the HIs. Due to their tensorial character, these interactions usually lead to complex dynamics, determined by the shape, orientation and relative velocity of the actors involved. Besides that, the induced displacements are largely affected by the presence of confining boundaries or external flows. Such complex interactions play an important role in a vast array of phenomena, including reproduction, bacterial infection, drug delivery or pattern formation in biological systems [7-10].

Despite this complexity, the laminar nature of the fluid flow at low Reynolds number (*Re*) makes the manipulation of colloidal particles easier, since the fluid does not present swirls or turbulences that may randomize their motion. The possibility of controlling HIs between colloidal particles is favored by our capability to trap, translate or torque colloids via external fields. The controlled motion of the colloidal particles in

the viscous medium enables the generation of stable flow patterns, suitable for their application in effective swimming strategies. These strategies are essential in the construction of microtransporters able to load and carry microscopic cargos, like cells, liposomes or microcapsules, in a noninvasive way, i.e. without the formation of irreversible bonds or the change of the chemical composition of the medium. The latter are compelling issues that must be faced for the design of new applications in lab-on-a-chip devices and biological systems. The hydrodynamic regime at the microscale facilitates, in some cases, the emergence of flow-induced bound and synchronous states, coordinated modes appearing in systems formed by interacting and rotating or oscillating entities [10-14].

In this work, we provide an overview on the current state-of-the-art in the use of locally generated hydrodynamic flows for swimming, transporting, and producing bound states that may show temporal synchronization. The review is organized in six sections. In section 2, we give a brief review of low *Re* hydrodynamics, avoiding rigorous formalism that can be found in textbooks [15-19]. In section 3, we describe the role played by HIs in diluted and dense colloidal systems, both in equilibrium and non-equilibrium conditions. In the fourth section, we explain the necessary requirements to achieve swimming at low *Re* and present a short outline of the main strategies adopted, focusing on those based on the local generation of flow fields. In the fifth section, we proceed by describing some experimental realizations that use different mechanisms for transporting passive objects at low *Re*. Finally, in the last section, we explain the role played by the HIs in the generation of bound and synchronous states, and we show some representative examples in colloidal and biological systems, where HIs lead to fascinating collective behavior.

2. The low Reynolds number (*Re*) regime

Colloidal particles have a typical size ranging from tens of nanometres to tens of micrometres. This characteristic length scale brings on the appearance of some distinctive features: (a) a high surface/volume ratio, that explains why the surface-chemical properties determine the stability of colloidal systems, (b) the relevance of thermal noise, and (c) the presence of interactions mediated by the dispersing medium, when the latter is stimulated by the motion of the dispersed particles [16]. The *Re* is a dimensionless quantity, used to characterize the flow motion, that does not only depend on properties of the medium, hereby the liquid density ρ and the dynamic viscosity η, but also on the size a and velocity v of the objects moving through the fluid,

$$\mathrm{Re} = \frac{\rho v a}{\eta} \quad . \tag{1}$$

In colloidal suspensions, inertial forces are negligible compared to viscous forces and the suspended particles move in an overdamped regime, where the applied forces and torques are constantly balanced by their viscous counterparts. Therefore, the *Re* is orders of magnitude smaller than in the macroscopic systems. In the absence of sources or sinks of flow, the motion of the fluid can be described by the Stokes equations

$$\begin{aligned} \nabla \vec{u} &= 0 \\ -\nabla p + \eta \nabla^2 \vec{u} &= -\vec{f}(\vec{r},t) \end{aligned} \quad , \tag{2}$$

where $p(\vec{r},t)$ is the dynamic pressure, $\vec{u}(\vec{r},t)$ the flow field, and $\vec{f}(\vec{r},t)$ the external body force field per unit volume [16, 20, 21]. The absence of the nonlinear convective acceleration and the time-dependent terms in these equations have two main consequences:

a) Navier-Stokes equations become linear. In steady fluids, the viscous torques and forces are proportional to the induced linear and angular velocities of the particles. Consequently, the flow field generated by a moving object, translating or rotating, is identical but oriented in the contrary direction to those generated by the reverse motion. On the other hand, the superposition principle applies, which means that the flow field at a given place and time caused by more than one actuation is the sum of the velocities that would have been provoked by each stimulus separately. The different flows are only coupled through the boundary conditions [22].

b) The Stokes equations are time reversible: the flow pattern is not modified by a reversing of the forcing, whether fast or slow. Time reversibility was nicely illustrated by G.I. Taylor with an experiment shown in the National Committee for Fluid Mechanics Film (NCFMF), named *Flow at Low Reynolds Numbers* [23], see schematic in Fig.1(a). The annular space between two concentric cylindrical containers is filled with a viscous fluid, and a coloured drop is injected in the fluid well away from the walls. If the inner cylinder is slowly rotated in one direction, it deforms and elongates the droplet. Afterwards, the cylinder is rotated in the opposite direction the same number of revolutions, till reaching its initial position. After these operations, the droplet recovers its initial shape, with small deviation due to the presence of diffusion.

In this low *Re* regime, we will now describe the flow due to a spherical particle dispersed in a quiescent fluid, and subjected to an external force. The force $\vec{F}(\vec{r}_j)$ exerted on the solid sphere j, and located at $\vec{r}_j$, creates a flow $\vec{u}(\vec{r}) = H(\vec{r} - \vec{r}_j)\vec{F}(\vec{r}_j)$ and a pressure field $p(\vec{r}) = \vec{g}(\vec{r} - \vec{r}_j)\vec{F}(\vec{r}_j)$ at $\vec{r}$, where the $H(\vec{r} - \vec{r}_j)$ and $\vec{g}(\vec{r} - \vec{r}_j)$ are

known as the Oseen tensor and the pressure vector, respectively. The flow generated by a moving particle can be calculated by solving the Eqs. (2) with a point force $\vec{f}(\vec{r}_j) = \vec{F}\delta(\vec{r} - \vec{r}_j)$ located at the particle's centre. Once the specific boundary conditions are satisfied, the viscous drag on a solid sphere is obtained by integrating the pressure tensor over its surface [16]. Applying no-slip boundary conditions, Stokes used this approach to obtain the flow field generated by a moving solid sphere of radius a, translating at a speed $\vec{v} = v\hat{z}$ through an otherwise quiescent fluid:

$$\frac{u_\alpha(\vec{r})}{v} = \frac{3a}{4}\left(\frac{\delta_{\alpha z}}{r} + \frac{z r_\alpha}{r^3}\right) + \frac{a^3}{4}\left(\frac{\delta_{\alpha z}}{r^3} - \frac{3 z r_\alpha}{r^5}\right). \quad (3)$$

Here $\vec{r}$ is the distance from the particle's centre and z the displacement along the direction of motion [24, 25]. At sufficiently large distances, the flow given by Eq. (3) is essentially independent of the sphere's radius.

Hence, in the limit $a \ll r$, the flow field around an isolated sphere continuously driven through a viscous fluid is equivalent to the flow generated by a unit force placed in the sphere's center. The corresponding Oseen tensor $H(\vec{r} - \vec{r}_j)$, called stokeslet, is the Green's function for the system:

$$G^S_{\alpha\beta}(\vec{r}) = \frac{1}{8\pi\eta}\left(\frac{\delta_{\alpha\beta}}{r} + \frac{r_\alpha r_\beta}{r^3}\right). \quad (4)$$

G^S is a good approximation for H when $r \gg a$, as confirmed when comparing Eqs. (3) and (4). The Stokes doublets (force dipoles), a different type of hydrodynamic singularities, are obtained by calculating the gradient of Eq. (4) in a given direction [26]:

$$G^{S}_{\alpha\beta\gamma}(\vec{r}) = \frac{1}{8\pi\eta}\left[\left(-\frac{r_\alpha \delta_{\beta\gamma}}{r^3} + \frac{3r_\alpha r_\beta r_\gamma}{r^5}\right) + \left(\frac{r_\gamma \delta_{\alpha\beta} - r_\beta \delta_{\alpha\gamma}}{r^3}\right)\right]. \quad (5)$$

The antisymmetric term in Eq. (5) is called a rotlet, and provides the velocity field corresponding to a rotational motion [27]. Thus, a small sphere subjected to a torque $\vec{T}$ rotates and generates a far flow field that decays asymptotically as $\vec{u} = \hat{T} \times \vec{r} / (8\pi\eta r^3)$, where $\vec{r}$ stands for the position vector from the particle's centre [28, 29]. The symmetric term in Eq. (5), known as stresslet, is often used to model the flow field generated by micro-organisms [30, 31]. Higher-order singularities (force quadrupoles, source dipoles, octupoles…) are easily obtained by subsequent differentiation. The schematics of some of these elemental singularity solutions are shown in Fig.1(b).

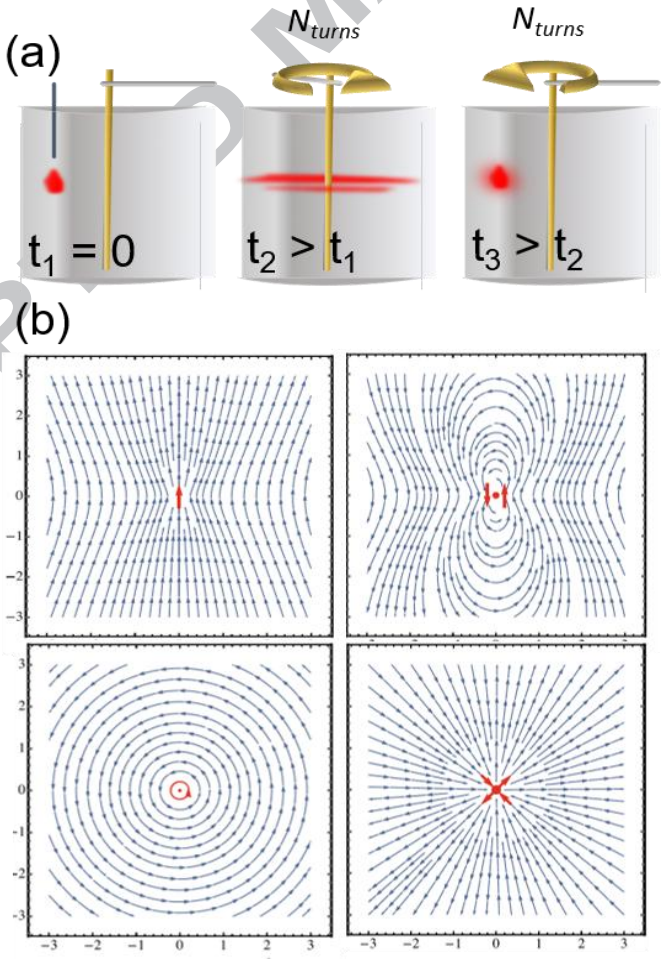

Fig. 1 a) Kinematic reversibility at low Reynolds number demonstrated by G. I. Taylor in the NCMF film *Flow at Low Reynolds Number*, Ref [23]. In this experiment, a coloured drop is injected in glycerine, filling the annular region between two concentric cylinders. By slowly rotating the inner cylinder in one sense for a certain number of cycles N_{turns}, and rotating in the reverse order till to the initial position, the droplet roughly recovers its initial shape. b) The flow field $\vec{u}(\vec{r})$ in the (x,y) plane for a set of singularity solutions: stokeslet (top, left), stokeslet doublet (top, right), rotlet (bottom, left) and stresslet (bottom, right). The hydrodynamic singularities are marked in red. [Figure (b) is reprinted with permission from Ref [32] (Copyright 2016 Springer)].

3. Hydrodynamic Interactions (HIs)

The flow excited by the random or driven motion of the particles in the fluid, modified by the presence of other particles or surfaces, transports energy through the dispersing medium [16, 30, 33, 34]. Therefore, particles present solvent-mediated forces, apart from other possible direct interactions such as steric, depletive, electrostatic, magnetic, etc... The flow field generated by an isolated object decays with the distance r as r^{-1} or r^{-2} and r^{-3}, depending if it is created by a driven or a force-free object respectively [30, 32, 35]. The flow velocity due to HIs between particles confined in 2D decays faster, at a rate of r^{-2} when the particles are driven by an external actuation [36]. At low *Re*, the HIs have a tensorial nature as they couple linear and angular velocity of the particles to forces and torques. Therefore, in contrast to electrostatic or dipolar interactions, HIs cannot be described by a simple potential term [15, 37]. If there are no external forces acting on the particles, then their motion is determined by the advection generated by the flow perturbations in the fluid (Faxén's law) and by the gradient in the velocity field, that tends to change the orientation of the particles.

HIs are fundamental in the equilibrium dynamics of colloidal systems. At low concentrations, HIs modify the effective diffusion coefficient of the particles [38-40], and lead to long-range correlations of the displacements induced by thermal fluctuations [41, 42]. On the other hand, the presence of an adjacent surface rectifies the flow generated by the particle motion, reducing its Brownian diffusion [43]. HIs play also a key role for the collective behaviour of crowded colloidal suspensions. Since at thermal equilibrium the average distance between particles is mainly determined by the potential energy, the HIs are expected to not have a significant role on the equilibrium structure of the system. However, HIs correlate the movement of the particles, and this effect has an important influence on the crystallization processes of colloidal systems, by shifting the freezing point to different densities [44]. By neglecting the HIs, it was shown that the attachment of particles to a growing crystal is a non-cooperative diffusive process, and the crystal nucleation rate is inversely proportional to the solvent viscosity. However, experiments disagree with the theoretical predictions and with the results obtained with computer simulations [45]. Radu and Schilling performed simulations of the crystal nucleation processes in colloidal suspensions of hard spheres, showing that the nucleation rate is enhanced by the HIs [46]. In contrast to hard spheres, colloids with screened Coulombic interactions displayed a reduction of the crystal growth velocity due to the effect of the HIs [47]. The role of hydrodynamic forces was also studied in the microphase formation of block copolymers, where Groot et al. showed how the HIs allow the system to overcome metastable states [48].

The most remarkable effects of the HIs, however, occur when colloidal systems are driven far from equilibrium [49]. Even under diluted conditions, the presence of HIs have important consequences on the dynamics of colloidal suspensions and biological systems. For example, the dynamic behavior of microparticles driven along an optical ring via a ratchet-like mechanism was largely altered by the HIs, and colloidal clusters

executed a caterpillar-like motion that enabled the surmounting of large potential barriers [50]. HIs have also a significant influence on the sedimentation of colloidal particles. When two spherical particles sediment in a viscous fluid, the leading particle drags the trailing one to the exact same extent that the other pushes it, so that the distance between the pair remains constant. The presence of an upper horizontal surface, however, breaks this spatial symmetry, causing the particles to experience a hydrodynamic force that draws them together [51]. The symmetry of the two-body HIs is also broken when the particles describe a circular trajectory [52], as shown in Fig. 2(b), by including a third particle that leads to a transient chaotic dynamics, Fig. 2(c) [22], or when both cases occur [53]. In practical applications, the flow generated by externally actuated microparticles was used to mix fluids, to build check-valves and fluidic pumps in lithographic structures [54, 55], Fig. 2(d), or in interfacial microrheological measurements [56, 57]. HIs also are believed to play an important role in the kinetic process of protein folding [58, 59], and they were proposed as potential actors in steering the ligand-protein binding [60].

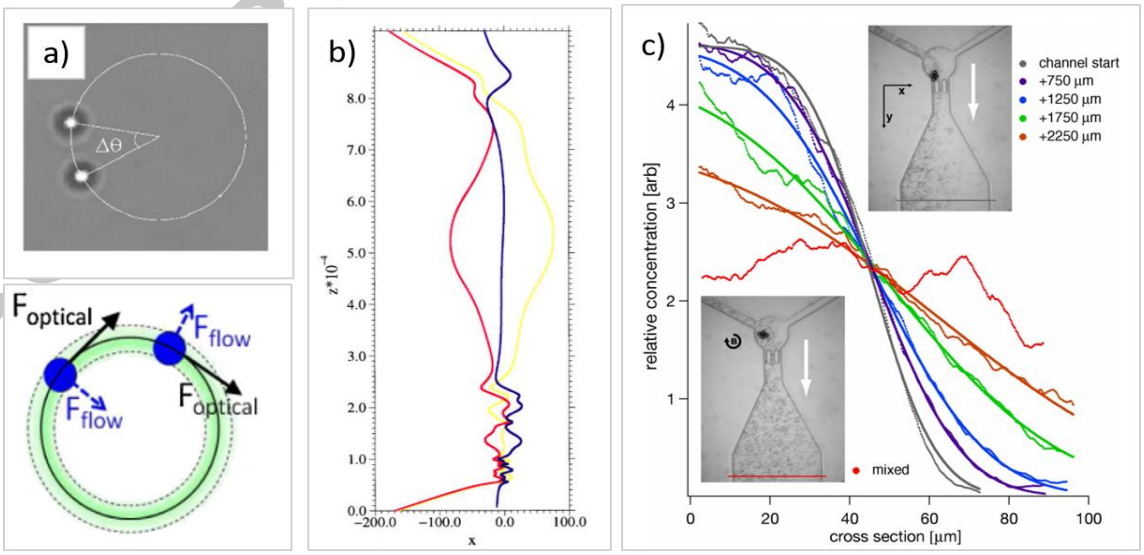

Fig. 2. Several effects of the HIs on the dynamics of relatively diluted colloidal systems driven out-of equilibrium. (a) Visualization of a pair of colloidal particles with an angular separation

$\Delta\theta$, steered through water by an optical ring trap. HIs pushed the leading particle outward and pulled the trailing one inward. (b) The chaotic motion of three hydrodynamically coupled particles slowly sedimenting through a viscous fluid. (c) Active mixer created via the assembly of magnetic colloidal particles under a rotating magnetic field. [(a) Reprinted with permission from ref. [52], (b) from ref. [22] (Copyright 2011 and 1997 APS) and (c) from ref. [55] (Copyright 2008 National Academy of Sciences)].

Beyond the very dilute limit, a long-standing debate has focused on understanding the role of HIs on the fluctuations of settling velocities in a suspension of sedimenting particles. In the absence of particle aggregation, hydrodynamic backflow causes a reduction of the settling speed from the velocity of an isolated particle [61]. Caflisch and Luke proposed that the velocity fluctuations arise from the balance between density fluctuations in the particle distribution and the Stokes drag, and they predicted that these velocity fluctuations diverge with the system size [62]. Other authors suggested that the long-range velocity fluctuations exhibit universal large-scale spatial and time correlations, when the suspension viscosity and sedimentation velocity are appropriately scaled with respect to the fluid viscosity and the average settling velocity [63, 64]. The latter assumption, however, contradicted both numerical studies and experimental observations that evidence a dependence of the velocity fluctuations on the container size and particle concentrations [65-67].

In another set of studies, it was shown that HIs have a large influence on the phase behavior of active colloids in two and quasi-two-dimensional confinement [44, 68], preserving the polar-liquid state from the characteristic density fluctuations frequently observed in populations of self-propelled particles [69, 70], Fig. 3(a), and avoiding the motility induced phase separation observed in different "dry" active systems [71-73]. In other systems, however, the role of HIs in motility-induced phase separation is currently unclear, since different experimental realizations arrive to apparently contradictory

conclusions, probably due to the effects of the near field interactions [74]. Furthermore, HIs had a large influence on the phase behavior of co-rotating hard disks two-dimensionally confined [37], Fig. 3(b).

HIs play an important role in the dynamics of gelation too. Furukawa and Tanaka, using numerical simulations, showed that the HIs significantly stimulate gelation in two and three dimensions, lowering the percolation threshold in suspensions of particles interacting though an attractive potential [75], Fig. 3(c). Due to the incompressible nature of the dispersing medium, particles may be subjected to hydrodynamic squeezing effects during the aggregation process. The resulting flow promoted the formation of elongated structures, enhancing the network-forming ability. HIs also are important in gelling systems where long-ranged repulsions are included. Direct interactions hindered the compaction of the clusters and induce the formation of elongated structures, being the percolation favoured by their anisotropic drag [76].

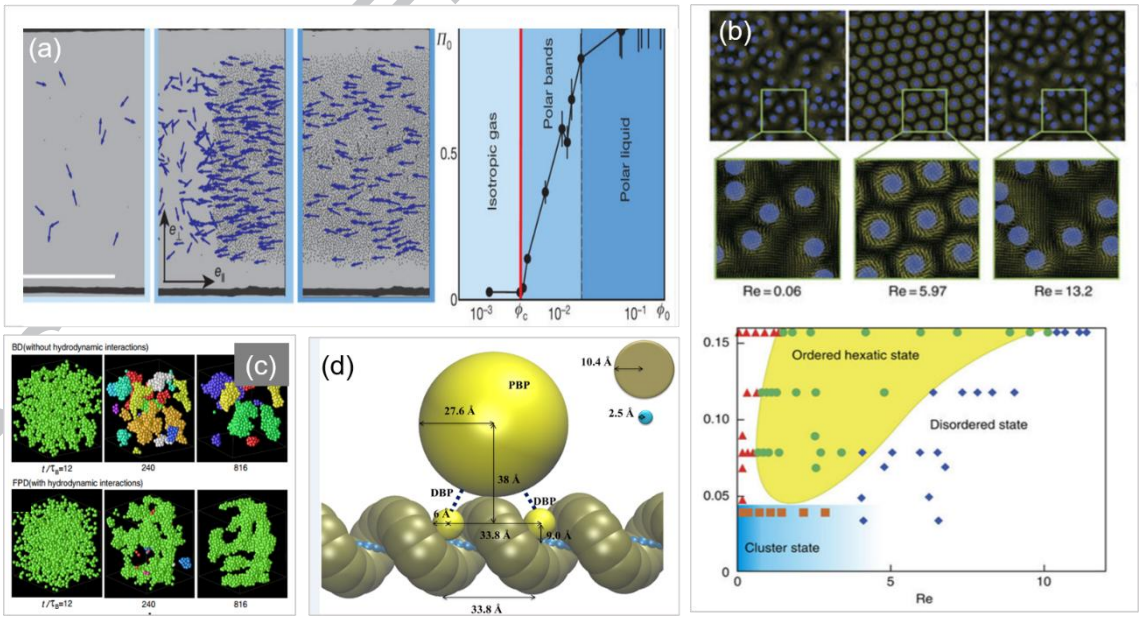

Fig. 3: Several effects of the HIs on the dynamics of concentrated colloidal systems driven out of equilibrium: (a) the formation and preservation of the polar-liquid state in populations of self-propelled colloidal rollers, characterized by the modulus of the average polarization Π_0, and

plotted vs plotted versus the area fraction ϕ_0, (b) the emergence of order states in a system composed by two-dimensionally confined rotating disks, and (c) the stimulation of the gelation process in suspensions of particles interacting though an attractive potential. (d) Schematic view of coarse grained protein and DNA models used for studying the effect that HIs have on the diffusion of the proteins along DNA molecules. [(a) Reprinted with permission from Ref. [69], (b) from Ref. [37] (Copyright 2013 and 2015 Nature Publishing Group), (c) from Ref. [75] (Copyright 2010 APS) and (d) from Ref. [77])].

Moreover, HIs play a fundamental role in a wide range of phenomena occurring in crowded biological systems. Some experiments show that HIs play a significant role in protein diffusion within cells at biologically relevant concentrations [78]. Computational techniques, frequently employed in the study of these complex biological systems, suggested that the diffusion of the proteins along DNA in the nucleoid is modified by the HIs [77], Fig. 3(d). Other important biologic phenomena that could be largely affected by the HIs are the dynamics of molecular motors [79], the kinesin walking along tubulin [80], the subcellular signaling [81], or the assembly of large scale molecular aggregates, such as the lipid bilayer [82], tubulin and actin filaments [83], to mention just a few examples.

4. Swimmers propelled via controlled hydrodynamic flows

Propulsion in viscous fluids plays a key role in many different contexts of biology, such as locomotion of microorganisms and reproduction. It is also important for different technological fields such as targeted drug delivery or microsurgery, in the creation of artificial swimmers and pumps, or the transport of nano-cargos through bloodstream or in microfluidic systems [84-87]. From a fundamental perspective, swimming in a viscous fluid presents the challenge of designing an adequate strategy capable to overcome the negligible role of the inertial forces as well as the randomization induced

by the thermal noise. The singular characteristics of the low *Re* number regime lead to the "scallop theorem", enunciated by E.M. Purcell forty years ago, which establishes a necessary but not sufficient condition for swimming: to avoid reciprocal motion, the latter being any periodic backward and forward body displacement [8]. This condition also reflects the requirement of having two separate degrees of freedom in the space parameter, able to trace a closed area. According to this argument, non-reciprocal swimmers reach their maximum velocity when, in the parameter space, the area covered by the trajectory of the deformations of the swimming cycle is maximized [88].

At low *Re*, particles can only be propelled by applying strategies based on non-reciprocal motions Fig. 4 (i and ii). Reciprocal actuations only are efficient in generating propulsion if the oscillating systems include some elasticity, in the swimmer, the medium or in an adjacent object, Fig. 4 (iii and iv) [7, 32]. On the other hand, in systems composed by a set of interacting particles there is no many-scallop theorem: two nearby particles undergoing reciprocal or nonreciprocal motions can propel cooperatively, in a collective fashion that depends on the sequence of the applied actuations [89].

In the last decade, different procedures for propelling microparticles in viscous fluids have been proposed. Significative examples include the generation of bubbles [90], self-acousto- or self-thermo-phoretic mechanisms [91, 92], and the applications of electric or magnetic field gradients [93-95]. In alternative approaches, the particles were chemically modified in such a way that they generate a flow field. For example, in catalytically powered Janus colloids [96-98], self-propulsion results from the catalytic generation of non-compensated hydrodynamic stresses along the particle surface [99]. In a pioneering experiment, Paxton et al. synthesized bi-metallic nanorods formed by a platinum and a gold segment. The Pt end catalyzed the decomposition of hydrogen

peroxide that in turn induced a fluid flow over the surface of the rod [100]. Since then, similar strategies based on the stimulation of asymmetric physico-chemical environments have been adopted in a great number of experimental systems [101]. Self-propulsion mechanisms break the time-reversal symmetry by continually generating entropy at a local scale.

Here, we will focus on micropropellers actuated by an external field, fundamentally different than reaction driven and biological microswimmers, which are force- and torque-free [30]. The lack of the autonomous character may be compensated by other advantages. The energy required for propulsion can be supplied to the particles on the fly by means of external fields, avoiding both the application of potentially harmful physico-chemical gradients (in temperature, pH, concentration of chemical compounds…) that are difficult to control, and the efficiency reduction due to fuel shortage and directional randomization.

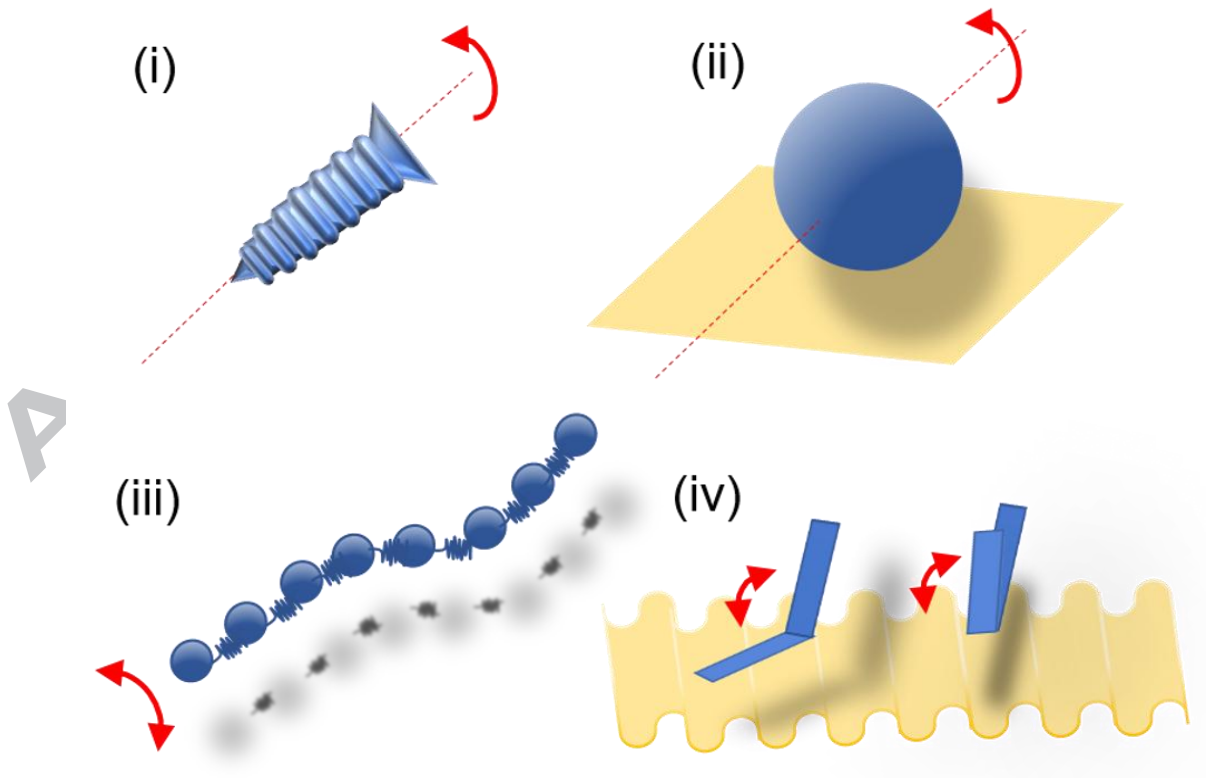

Fig. 4. Different strategies used for propelling actuated particles through a viscous fluid: by rotating a chiral object in the medium (i), or spheres in the proximity of a boundary (ii), and by inducing the reciprocal motion of flexible structures (iii), or rigid structures near a flexible surface (or a viscoelastic medium) (iv).

4.1 Torque-driven non-spherical swimmers

We previously showed that in the Stokes regime the applied forces and torques are related to the linear v and angular ω velocities. In the one dimensional case, when the motion of the actuated swimmer can be described only by the rotation and translation along a unique axis, the previous magnitudes are connected through a 2×2 symmetric resistance matrix P [8]:

$$\begin{pmatrix} F \\ \tau \end{pmatrix} = P \begin{pmatrix} v \\ \omega \end{pmatrix} = \begin{pmatrix} LA & L^2C \\ L^2C & L^3D \end{pmatrix} \begin{pmatrix} v \\ \omega \end{pmatrix}, \tag{6}$$

where L is a characteristic dimension of the propeller, and A, C and D are parameters that, for a fixed axis of rotation, only depend on the fluid viscosity and the propeller shape. For a homogeneous spherical object, P is diagonal and the external torque is not linked to the linear velocity. Therefore, propulsion is not possible by rotating a colloidal sphere in the bulk of the fluid [84]. The breaking of the spherical symmetry, however, makes P non-diagonal, allows rotation-translation coupling and thus the possibility of inducing propulsion through an external torque. As stated by Purcell: "Turn anything – if it isn't perfectly symmetrical you'll swim" [8]. In most of the designs, torque-driven propellers were based on helical shapes, which display a motion like that of a corkscrew burrowing into the viscous fluid [84, 102-105], Fig. 5(a). As in the case of the corkscrew, the rotation must have a defined chirality, since alternating rotational modes could be perfectly balanced, and thus not lead to any translation, but only to an enhanced diffusivity [106]. Usually, these helicoidal

structures are ferromagnetic, with a magnetic moment oriented orthogonally to the long axis. Thus, a rotating magnetic field applies a torque along its main axis. These prototypes mimic some existing natural systems. For instance, in some bacteria the propulsion is induced by the rotation of one [107] or various helically shaped flagella [108, 109], torqued by a molecular engine [9, 110], Fig. 5(b). The multiple flagella are often concentrated at one end of the bacteria's bodies, and the complex effect of their bundling has been studied in a model system composed by rotating macroscopic helical wires in a highly viscous fluid [111]. In the artificial helical swimmers, the pitch of the helix is an important geometrical factor: swimmers characterized by longer pitches feature better propulsion performance, provided that the number of turns is kept constant [112]. Helical microswimmers can serve as near-term goal for numerous wireless tasks, ranging from in vitro cell characterization to in vivo applications for diagnosis and minimally invasive therapies [85]. The helicoidal shape, however, is not mandatory for coupling rotation and translation. The loss of spherical symmetry is enough, and achiral and arbitrarily shaped structures were used for getting rotation-translation coupling [113, 114], Fig.5(c). Indeed, swimmers consisting of slender bodies with a single centerline were proposed as optimal designs [115].

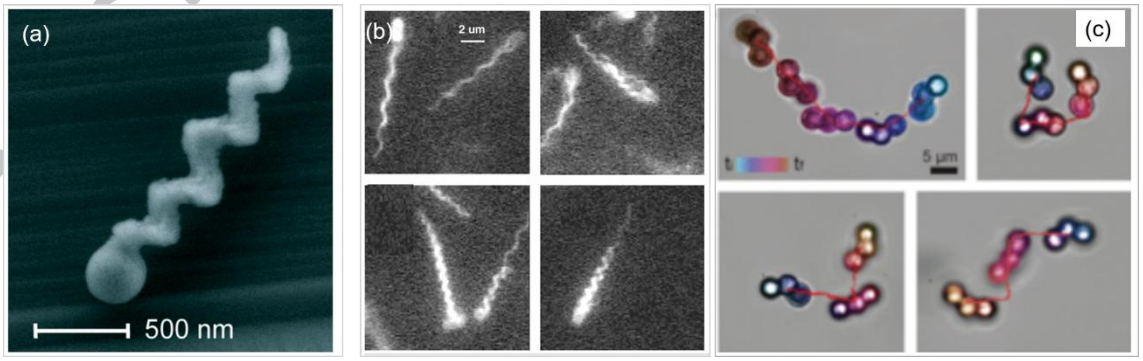

Fig. 5. Different designs for propelling torque-driven objects through a viscous fluid: (a) Ferromagnetic helically shaped flagella burrow into the viscous fluid driven by an externally applied rotating magnetic field. (b) Cells of Escherichia coli bundle various rotating flagella for

adopting the helicoidal geometry. (c) Achiral structures displaying rotation-translation coupling [(a) Reprinted with permission from Ref. [104] (Copyright 2009 ACS), from Ref. [109] (Copyright 2000 American Society for Microbiology) and from Ref. [113], (Copyright 2014 APS)].

4.2 Torque-driven swimmers close to a boundary

The presence of a nearby surface has a strong influence on the dynamics of propelling systems. For example, surface-mediated HIs can be used for steering the propellers along defined trajectories [116], explain the attraction of some swimmers toward an interface [117], the circular path shown by E. coli [118] or the rectification of rotation into translational motion [28]. At low *Re* rotation can be rectified into net translation due to the HIs with the near interface, that depending on its nature imposes one or another boundary condition [119]. Blake, by generalizing the Lorentz's ideas, suggested that the flow generated by a moving particle near a surface could be calculated by placing a set of hydrodynamic images, so that the corresponding boundary condition could be satisfied along the interface [26, 120]. The effect of a flat surface on the flow generated by a translating or rotating sphere, located at a distance h from the surface, can be accounted through an appropriate set of hydrodynamic singularities located at the same distance h but on the opposite side of the interface. The choice of the set of singularities does not only depend on the geometric configuration, but on the specific boundary conditions that constrain the fluid flow field at the bounding interface. The hydrodynamic image of a stokeslet in the presence of a stationary no-slip wall is not simply another stokeslet, but a combination of an oppositely directed stokeslet (S), a stokes dipole (D) and a source dipole (SD) (a sink and a source brought together) [26, 120]. According to the previous model, the mobility of a driven sphere decreases near a wall, being larger along the interface, than perpendicular to it [30]. On the other hand,

the image of a rotlet driven by a torque $\vec{T}$ near a stationary liquid-gas interface, where slip boundary conditions hold, reduces to a particle rotating in the opposite sense than the real particle, actuated by a torque $\hat{T}^* = -\eta\hat{T}/\eta_g$, where η_g is the gas shear viscosity [26]. For a liquid-solid interface, where stick boundary conditions are satisfied, the image system consists of a linear combination of a rotlet, a stresslet and a source doublet [27]. In the latter case, the torque acting on the image has the same magnitude that the torque actuating on the deposited particle $\hat{T}^* = -\hat{T}$ [28]. For an isolated and torque-driven particle placed at a distance h above the surface, the component of the flow velocity parallel to the surface is $v_0 = {}^{Ta^2}\!/_{(32\pi\eta h^4)}$ for liquid-solid interface, and $v_0 = {}^{-T}\!/_{(32\pi\eta_g h^2)}$ for a liquid-gas interface. In both cases, propulsion is induced by the flow generated by the image singularity, which has a component parallel to the interface at the particle's center. According to the last equations, when comparing propulsion between identical rotors in the proximities of solid or liquid surfaces, one can expect both the increase in the magnitude of the speed of a rotor in the presence of a liquid-gas interface and the change in direction with respect to the solid-liquid interface [28]. In contrast to rotating spheres, a rotating cylinder laying on the surface does not display translational motion since the viscous stress is balanced by the dynamic pressure field [121].

In most of the cases, the microrotors are particles having a permanent magnetic moment made up of ferro- or antiferromagnetic materials, or paramagnetic colloidal particles [14, 28, 122]. In the latter systems, the field induced magnetic moment is supposed to be parallel to the field itself, and consequently spherical particles actuated by a rotating field should not present any induced torque. However, the rotation may be induced by other mechanisms as internal relaxation effect of the particle magnetization [123]. Janssen et al. measured the field induced rotational motion of paramagnetic colloids and

explained this magnetic relaxation in terms of the presence of small permanent magnetic moments in the particles, non-detectable by means of vibrating sample magnetometry, and the complex nature of the magnetic susceptibility of the particles [124]. In the case of ferromagnetic colloids, the rotation behavior can be discriminated in two different regimes, delimited by a critical field frequency. At relatively low frequency, the particles rotate synchronously with the applied field. Above the critical frequency, the system enters a second asynchronous regime, where the viscous force, proportional to the angular velocity, equals to the exerted magnetic torque, and particles cease to rotate at the frequency fixed by the field [4, 124].

The rotation-translation coupling strategy has been explored by different groups for moving force-free micro-rollers [54]. Janus particles [125] and anisotropic hematite particles [126], were transported under the action of a rotating magnetic field via hydrodynamic surface effects. The field induced tumbling motion of Ni ferromagnetic nanowires also leaded to propulsion when located near a substrate [127]. More complex structures were precisely transported by taking advantage of the hydrodynamic coupling with the close surface. DNA-linked doublets made up of paramagnetic microparticles were propelled in a viscous fluid when subjected to a precessing field in the proximity of a solid boundary [4, 128, 129], Fig. 6(a).

Also unbounded chains were driven in a viscous fluids by a rotating magnetic field: dynamically self-assembled colloidal linear aggregates “walked” along planar surfaces in a viscous fluid [130], Fig. 6(b), and microscopic “worms”, dynamically assembled by elliptically polarized rotating magnetic fields, were propelled on a plane due to the cooperative flow generated by the constituent rotating particles [28], Fig. 6(c). In the latter case, the one-dimensional chain was modeled as a chain of rotors near a surface, and it was found that the linear velocity of the worm increases with the number of

particles, till reaching a saturation value at a given worm length. The worms were observed to propel in opposite directions when placed at a gas/liquid or a solid/liquid interface, since the local flow induced by the stick boundary condition characteristic of the solid wall differed from the one generated by the slip boundary condition imposed by the liquid-air interface. Analogously, the presence of a surface was used in Ref. [131] to reverse the rotation of *E. coli*. Similar strategies were adopted for propelling linear ribbons composed of paramagnetic spheres [122], or ferromagnetic microellipsoids that arranged with their long axis parallel to each other [132, 133], all of them torqued by magnetic fields. In the latter case, the flow was generated by linear arrangements oriented parallel to the axis of rotation and perpendicular to the direction of translation. In the latter case, the flow generated by the rotating particles, and rectified by the nearby interface, did not present a component in the direction of the motion along the ribbon. Hence, in contrast to the self-assembled microscopic worms of Ref. [28], the constituent ellipsoids were not advected by the flow generated by the rest of rotors, and the velocity of the ribbons did not present any dependence with length. In all those driven systems, the propulsion speed was regulated by varying the driving frequency, or the torque via the field strength. By applying a dynamic 3D magnetic field, and using the same hydrodynamic mechanism previously described for propelling the worms, paramagnetic microrotors assembled into highly ordered two-dimensional carpets were manipulated and propelled [14], Fig 6(d). Although the speed acquired by an individual rotor moving close to the interface was relatively slow, for an ensemble of rotors forming the carpet the effect became cooperative, resulting in a faster translational motion.

Surface rotors are suitable to work in confined geometries such as microfluidic channels or biological networks characterized by narrow pores, and the hydrodynamic conversion of collective rotations to net translational motion was described in an ensemble of

rotatory motors confined to straight and ring channels [134], Fig. 6(e). These operations are possible unless the rotors are placed in the channel centre, where they display the same distance between the top and the bottom surface. In the latter case the hydrodynamics forces are balanced.

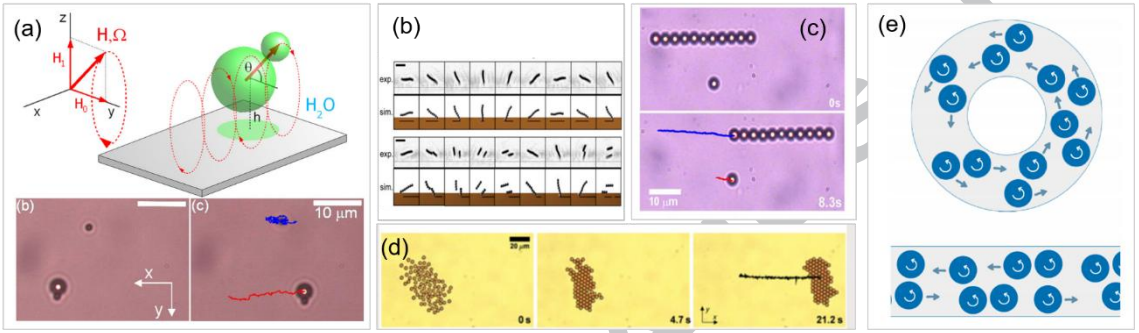

Fig. 6. Different designs for propelling torque-driven confined objects: (a) Permanently linked paramagnetic colloids, propelled in water by a precessing field in the proximity of a wall. (b) Sequence of images showing dynamically self-assembled linear aggregates of paramagnetic colloids subjected to a rotating magnetic field and "walking" along a solid boundary in water. (c) Magnetically assembled aggregates formed by rotating entities translating on a glass surface due to a cooperative hydrodynamic flow. (d) Sequence of images showing carpets made up of paramagnetic microrotors and transported under the action of a dynamic magnetic field. (e) Coupled rotation-translation in confined collections of rotatory particles. [(a) Reprinted with permission from Ref. [128] (Copyright 2008 APS), (b) from Ref. [130] (Copyright 2009 National Academy of Sciences), (c) from Ref. [28] (Copyright 2015 APS) (d) from Ref. [14] (Copyright 2015 APS) and (e) from Ref. [134] (Copyright 2011 IOP)].

4.3 Flexible swimmers

The controlled actuation of flexible filaments in viscous medium has been used in different designs for artificial microswimmers. These prototypes take advantage of the motion of slender filaments with drag anisotropy, which generates forces perpendicular

to the local direction of motion. The origin of this hydrodynamic anisotropy has been explained in terms of the resistance matrix of a slender rigid rod, of radius a and subjected to an external force $\vec{F}_{ext}$, by using a far field approximation similar to the one described in Section 4.2, where the motion depicted by chains of rotors was modelled by a set of equidistant rotlets. Assuming a uniformly distributed force, and disregarding internal cohesive forces, one assumes that the stokeslet contributions dominate over that of the other singularities. Thus, the rod is modeled as N parallel and equally spaced stokeslets [27, 30]. Applying the superposition principle, the velocity of each segment is calculated from the sum of the flow induced by the external force above all segments composing the rod, Equation (4). In the continuum limit the sum is replaced by an integral. Neglecting end effects and considering that in a rigid rod all the segments have the same velocity, the resistance matrix presents the well-known dependence on the rod length L [30, 135]. In this model, the flow field generated by an external force is half in the perpendicular than in the parallel direction. Due to the drag anisotropy, a rod or an ellipsoid subjected to a constant force not applied along any principal axes will move in a direction different to that imposed by the force. This fact explains the tilted fall of a cylinder under gravity in a quiescent fluid [23, 136]. According to the previous argument, the anisotropy in the mobility matrix is reminiscent of the anisotropy in the mobility matrix resulting from the stokeslet solution given by Equation (4).

The drag force on an oscillating filament, regarded as a set of slender segments moving with velocity $\vec{u}(\vec{r},t)$, also presents a component perpendicular to the direction of the velocity in each infinitesimal section, see Fig. 7(a). The drag per unit length on the filament includes a propelling component in the direction of phase propagation,

$$\vec{f}_{prop} = (\xi_{\parallel} - \xi_{\perp}) u \sin\theta \cos\theta \hat{e}, \tag{7}$$

where $\xi_{\parallel}$ and $\xi_{\perp}$ are the resistive coefficients parallel and perpendicular to the local tangent, and θ is the angle between the direction of motion and the local tangent [30, 84, 137]. Since the hydrodynamic forces are symmetric around the axis of oscillation, the object is propelled in the direction determined by the main axis of symmetry. In a time-periodic motion, the propelling force acting on the whole filament is only non-zero if $\theta(\vec{r},t)$ varies in time, i.e. when the filament is flexible [137]. In order to break the time reversal symmetry, a filament causes different undulating deformations [138], and the propulsion can be significantly enhanced by varying the flexibility along the filament [139]. The variation in $\theta(\vec{r},t)$ implies that the filament is flexible, but not necessarily elastic. In fact, most theoretical treatments of the dynamics of filaments use resistive-force theory [140], or more accurate slender-body theories [141, 142], without incorporating the elastic response of the filament [143, 144]. The elastic nature has been included by using Kirchhoff rod theory for the filament [143, 145], or approximating the filament as a network of springs [146]. More recently, the propulsion of an elastic filament has been modeled using the discrete elastic rods (DER) method [147], but calculating the hydrodynamic forces with the Lighthill's slender body theory [142, 144]. Flexible anchored cilia were also modeled by small spheres moving close to a planar surface on an elliptic and tilted trajectory, which reproduced the path followed by the center of mass of the cilia that deform their shape by breaking the symmetry of their stroke and thus satisfying the condition imposed by the scallop theorem. The far flow field generated by each sphere was described by Vilfan et al. through a stokeslet and an image mirrored over the boundary plane, consisting of a combination of an oppositely directed stokeslet, a stokes dipole and a source dipole [148].

Different force-free microswimmers have been designed by taking advantage of synthetic flexible filaments that can be deformed in a continuous manner. The first

flexible micro-swimmer, constructed by attaching a DNA linked chain of paramagnetic colloidal particles to a red blood cell, was propelled by applying a sinusoidal superimposed onto a constant magnetic field [149, 150]. This torque-driven swimmer resembles spermatozoa and eukaryotic cells. However, in this kind of swimmers the direction of propulsion is determined by the filament properties. While the induced waves propagated from tail to head in the artificial design, propelling the object in the direction towards the free end, most of the microorganisms display the opposed behavior. Propulsion of flexible helical rods rotating in a viscous fluid has also been widely studied [144]. Torque-driven propulsion of flexible nanowires, with a gold head and nickel tail and linked by a flexible silver bridge, was realized by applying a rotating magnetic field. In this prototype, the direction of motion was determined by the relative size of the gold and nickel segments [151], see Fig. 7(b). A different kind of flexible nanomotors, made up of a Nickel micro-head and a flexible Ag tail, was propelled by a precessing magnetic field, with a component rotating in a plane perpendicular to the constant component [152]. In this study, the propulsion mechanism was based on the chiral deformation along the flexible filament, as demonstrated by symmetry arguments. In contrast to the rigid chiral objects, these flexible propellers exhibited swimming in only one sense, independently of the rotational direction imposed by the external magnetic field.

Propulsion in force-free microswimmers was also demonstrated in non-Newtonian fluids, where the scallop theorem no longer holds [153, 154]. These designs achieved propulsion via reciprocal motion, exploiting the elasticity and the strain rate-dependent viscosity of non-Newtonian fluids, see Fig. 7(c). In those systems, propulsion was favored or hindered by the increase on elasticity, depending on the swimmer structure, the motion strategy and other nonlinear effects [153]. Reciprocal movement can also be

used for translating if this motion is performed in the proximity of a deformable interface [35, 155], see Fig. 7(d).

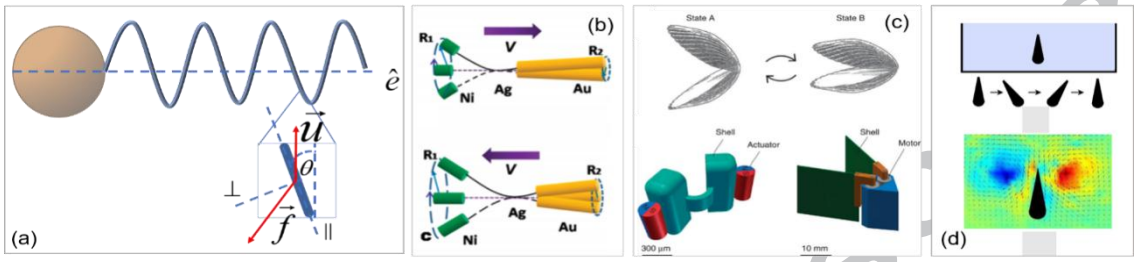

Fig. 7. Different strategies used for propelling at low Reynolds number, taking advantage of the elastic properties of the swimmer or the medium. (a) A flexible filament undulating vertically and sinusoidally. Here, each infinitesimal section is regarded as a slender segment oriented along θ and displays a component of the drag force $\vec{f}$ perpendicular to the direction of the imposed velocity $\vec{u}$. (b) Torque-driven propulsion of a flexible nanowire made up of a gold head and nickel tail, linked by a flexible silver bridge. (c) An artificial microswimmer propelling in a non-Newtonian fluid via a reciprocal actuation. (d) The reciprocal motion is also effective for propelling when it is performed near a flexible interfase. [(b) Reprinted with permission from Ref. [151] (Copyright 2010 ACS), (c) from Ref. [154] under a Creative Commons CC-BY license, and (d) from Ref. [35] (Copyright 2008 APS)].

5. Hydrodynamic transport of microscopic cargo

There is an increasing interest for technological applications capable of transporting on command cargos, colloidal particles or biological entities, like cells, in viscous and biological fluids. Thus, in last decades, different successful approaches have been realized. One of them relayed on the use of self-propelled catalytic microdockers to transport silica, polystyrene, and TPM (3-methacryloxypropyl trimethoxysilane)

particles [156], biological cells [157], or a large number of polymeric objects [158, 159]. Other strategies used symbiotic combinations of different methods: Janus particles were self-propelled by the decomposition of hydrogen peroxide on the metal caps, transporting magnetic particles loaded via field induced magnetic interactions [160], and rotating particles pushed and pulled microcargos thanks to the simultaneous use of hydrodynamic and phoretic interactions [126]. Other authors used gold nanowires to transport tumor-necrosis factor-alpha, by means of electrophoretic and dielectrophoretic forces [161]. Optical traps requiring laser beams, transparent samples, and typically generated in the proximity of a microscope objective, made it possible to trap and reconfigure many cargos in the microscale with dynamic patterns [1, 162]. Light was also used as a driving mechanism in different systems based on phototaxis, where the cargos were transported and released by means of colloidal particles [163], or motile microalgae [164]. An alternative non-contact strategy was the use of acoustical tweezers that generated trapping forces based on the difference in compressibility between the cargo and the medium [165]. Nickel-embedded nanotubes, used for molecular delivery into mammalian cells [166], or magnetic particles, employed to characterize the mechanical behavior of DNA [167], were positioned in three dimensions by the action of magnetic field gradients, a technique dubbed magnetic tweezers. In more atypical approaches, paramagnetic colloidal particles were steered on uniaxial magnetic garnet films in order to realize transport [168] and/or micro-sieving operations [169], and motor protein-based microdevices consisting in kinesin-coated microbeads were transported across arrays of microtubules [170].

The trapping, transport and positioning of microspheres in microfluidic systems via externally induced hydrodynamic flows was also demonstrated in different works. These strategies do not require direct contact with the sample, and thus limit its damage in contrast to other techniques that involve high intensity lasers, chemical bonding or

strong electric fields, experimental conditions that are usually non-desirable in the study of many biological samples [6]. Vortex-induced trapping provides promising approaches for high-throughput size-selective separation of cells and particles. In the intermediate Reynolds number regime, inertial forces are effective, and suspended particles can enter the induced vortex, where they become trapped within the recirculation zone [6, 171-175]. In other approaches, advective flows created through optical scattering in non-absorbing liquids were used to impart forces to the surrounding colloidal medium [176].

The generation of controllable and mobile hydrodynamic vortices able to trap small microobjects is a difficult task at the microscale, but it was recently demonstrated with helical micromachines consisting of a helical body and a microholder head [103], Fig. 8(a), as well as artificial flagella attached to a solid surface and actuated in a nonreciprocal manner by an external field [177, 178]. An alternative strategy to advect cargos through the generated flow is to induce the rotation of actuated micromachines in the presence of an external interface. Nickel nanowires and self-assembled magnetic bead doublets, rotating near a solid surface and inducing mobile microvortices, showed potential for targeted drug delivery, cargo transport and cell manipulation [127, 179]. In previous Section 4.2, we showed how, in the proximity of a flat boundary, a worm made up of an array of rotating particles generated a cooperative flow field in a direction perpendicular to the rotation axis [28]. This flow field was used for transporting nonmagnetic particles, which were continuously trapped in a hydrodynamic conveyor belt, see Fig. 8(b). Once close to the moving chain, the passive particles were captured by the hydrodynamic flow and rapidly dragged along the worm till they were expelled at the front. The relatively small cross section of the linear worms, however, hindered the load and transport of cargos larger than 3 microns. To solve this contingency, the torque driven rotors composing the worm were rearranged in a more extended 2D

configuration by applying a dynamic 3D magnetic field. These self-assembled 2D carpets, composed by paramagnetic microspheres, transported microscopic cells over its upper surface by using the hydrodynamic flow generated by the rotating particles [14, 180]. The loading of the cargo was done by direct entrapment or by lifting the cargo when the carpet moved or rotated close to it. Cooperative flows were also generated and used to transport large vesicles by the walkers described in reference [130]. In colloidal suspensions composed by antiferromagnetic rollers, hydrodynamically induced fingering instabilities were used to advect passive particles [13], see Fig. 8(c), and self-assembled ribbon-like structures translating perpendicular to the ribbon main axis, pulled or pushed non-magnetic cargos on a solid surface [132]. In the latter design, colloids were repelled or attracted by the ribbon depending if those were in front of or behind the propelling chain respectively. This behavior is not surprising, since in the low *Re* regime the reversal of external non-hydrodynamic torques induces a reversal of the motion of fluid and particles. Employing similar hydrodynamic approaches, individual micro-objects were effectively entrapped and transported at low velocities by the hydrodynamic flows generated by annular structures [181], see Fig. 8(d), and magnetic microlassos [182], see Fig. 8(e). Non-rotational motions were also used for inducing the motion and the transport of objects in the proximity of a boundary. Ferromagnetic composite microdockers resting on a solid surface presented a controllable stick-slip motion under the influence of time-varying magnetic fields, and served as transporters of single cells [183]. Finally, it is worthy to mention that mechanisms of transport based on advection are ubiquitous in biological systems. At the cellular scale, molecular motors induce passive advection by intracellular flows of bulk cytoplasm, a phenomenon known as cytoplasmic streaming [184]. In some cases, cytoplasmic flows are due to forces that come from the motion of the transported cargo

itself [185]. At the extra-cellular scale, the collective whip-like motion of cilia propels the fluid along the surface of cells, channels and tissues [186, 187].

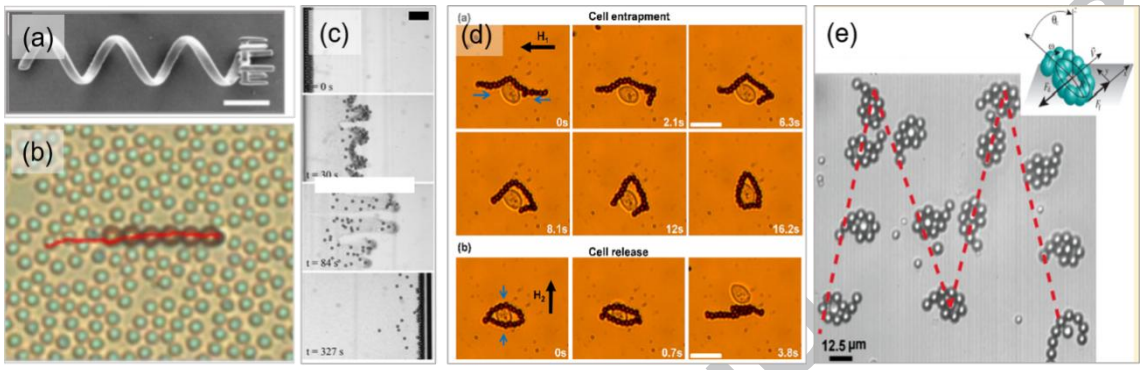

Fig. 8. Different strategies designed for transporting objects in a viscous fluid at the microscale by using HIs. (a) Helical micromachines demonstrated cargo transport of microparticles in 3D. (b) Silica particles were advected on a colloidal worm composed by a set of equally separated magnetic rotors. (c) Passive particles were transported by hydrodynamically induced fingering instabilities. (d) Yeast cells were transported and delivered by fragile magnetic rings, composed of rotating magnetic ellipsoids. (e) Passive particles collected and transported by hydrodynamically propelled colloidal microlassos. [(a) Reprinted with permission from Ref. [103] (Copyright 2012 Wiley), (b) from Ref. [28] (Copyright 2015 APS), (c) from Ref. [13] (Copyright 2016 Nature Publishing Group), (d) from Ref. [181] (Copyright 2016 APS) and (e) from Ref. [182] (Copyright 2017 ACS)].

6. Hydrodynamic Bound and Synchronous States

The dynamics of an ensemble of driven particles are governed by the interplay between the direct interactions, the thermal noise, and the HIs coupled with the dispersing medium. In some cases, the HIs are the main responsible for the appearance of self-organized states where few or more particles have the tendency to remain aggregated for a certain period of time. In Section 3 we already mentioned that HIs lead to long-

range hydrodynamic correlations of the particles' Brownian motion [41, 42]. Apart from the correlations between longitudinal position, HIs mediate the transverse fluctuations as well as the orientation of one particle and the displacement of its neighbor perpendicular to the interparticle direction [15, 33, 42, 188, 189]. On the other hand, three particles initially disposed in a horizontal equilateral triangle sediment in such a way that their trajectory is a simple periodic function of time [190], and two spheres driven along a circular path by an optical ring trap coupled due to the HIs [52], as we mentioned in Section 3. In the latter experiment, the increase in the number of particles driven around such an optical trap stimulated the appearance of hydrodynamically sustained vibrational modes, creating an underlying configuration of equidistant dimers [191]. The complex HIs between rotating particles lead to different dynamical regimes, depending on the system parameters. As demonstrated in Ref. [192], a couple of rotating disks, separated at a fixed distance and confined to two dimensions, presented HIs that lead to the rotation of the motors around each other, when spinning in the same sense, and to translation at constant velocity, when spinning in the opposite sense. Two counter-rotating spinners generated attractive flows, whereas particles rotating in the same direction displayed a hydrodynamic repulsion. This repulsive interaction became attractive when the rotating particles are embedded in a dense monolayer of non-actuated colloidal particles [29]. The balance between magnetic attractive interactions and hydrodynamic repulsive interactions emerging between rotating disks, floating at a liquid/air interface, leaded to the assembly of Wigner crystal states [193, 194]. HIs also lead to the emergence of coordinated, cooperative motion and self-organization in assemblies of non-actuated particles [195, 196] or motile organisms [197, 198]. They played a determining role in the swarming behavior of different micro-organisms, generating different patterns composed by swimming bacteria [198], and confined arrays of spermatozoa, with significantly increased motility [199].

Self-propelled organisms are often described through a simplified hydrodynamic model, the squirmer, introduced first by Lighthill [200] and later by Blake [201]. A spherical squirmer of radius a is defined as a propeller that performs axisymmetric distortions on its surface. If the surface of the spherical squirmer deforms steadily and only along the tangential direction, then in a co-moving frame the radial and tangential components of the fluid velocity are respectively given by:

$$\begin{aligned} v_r(r,\theta) &= \frac{2}{3}\left(\frac{a^3}{r^3}-1\right)B_1P_1(\cos\theta)+\sum_{n=2}^{\infty}\left(\frac{a^{n+2}}{r^{n+2}}-\frac{a^n}{r^n}\right)B_n(t)P_n(\cos\theta) \\ v_\theta(r,\theta) &= \frac{2}{3}\left(\frac{a^3}{2r^3}+1\right)B_1V_1(\cos\theta)+\sum_{n=2}^{\infty}\frac{1}{2}\left(n\frac{a^{n+2}}{r^{n+2}}+(2-n)\frac{a^n}{r^n}\right)B_n(t)V_n(\cos\theta) \end{aligned}, \tag{8}$$

where r is the distance to the squirmer's center, θ is the azimuthal angle measured from the direction of motion, $P_n(\cos\theta)$ are Legendre polynomials of order n, $V_n(\cos\theta)=\frac{-2}{n(n+1)}\partial_\theta P_n(\cos\theta)$, and $B_n(t)$ are coefficients with dimensions of velocity [202]. In the far field, when $r \gg a$, the series above are often truncated at $n=2$. Defining the parameter $\beta = B_2/|B_1|$, squirmers can be classified as pullers ($\beta>0$), pushers ($\beta<0$) and neutral swimmers ($\beta=0$). As shown in Fig. 9(a), pushers have their active propelling part on their rear side, pushing fluid from the body along the direction of locomotion and drawing fluid in to the sides, whereas pullers present the same streamline pattern as that for pushers, but with the reversed flow direction [32]. Squirmers are widely used as simplified model systems to study the role played by the HIs on the collective motion of biological systems. Two side-by-side pushers attract each other, while two side-by-side pullers repel each other [30, 203]. Pullers approaching on a converging path induced attracting flow fields on each other that reoriented them in the main component of locomotion, whereas under the same conditions pushers arranged in a side-by-side configuration [30, 32]. In the case of

pushers, however, the HIs at short range lead to the instability of the side-by-side configuration and to unsteady three-dimensional trajectories [30, 204]. Hence, a linear chain of pullers is stable while a chain of pushers gradually disaggregates as the propulsion velocity increases [205]. In bulk and non-diluted conditions, squirmers with $0 < \beta < 1$ do not exhibit phase separation but a polar order [206]. Shashi et al. found that squirmers formed ordered rafts, with a hydrodynamic induced correlation extending over more than four particle diameters [207]. When confined in a monolayer, the squirmers were observed to form various types of coherent structures, gas-like, cluster phases and hexagonal cluster states generated by HIs [68, 208]. In those systems, the collective behavior was crucially dictated by the balance between the near field hydrodynamics, the self-propelling mechanism, and the confinement [209].

Confinement has a strong influence on the dynamics of self-propelling systems interacting via HIs [210]. Close to a planar surface, pairs of dancing volvox orbited each other due to the interplay between short-range lubrication forces and solvent mediated forces [211], Fig. 9(b). At relatively high densities spermatozoa self-organized into dynamic vortices mediated by the HIs [10]. In the previous Section 4.2, we described the propulsion mechanism used by hematite micro-rotors for propelling above a flat surface [126]. These microrotors exhibited long-living hydrodynamic bound states, where the particles aligned along their long axis during propulsion or along a finite angle, and adjusted their speed by slowing down or speeding up due to the generated flow field [212]. The emergence of these coupled trajectories was explained considering the HIs with the boundary surface and the effect of gravity, and in dense suspensions, these hydrodynamic bound states can be extended to one dimensional arrays of particles. With other type of magnetically torqued particles, here polystyrene microspheres with a protruding ferromagnetic cube, HIs where found able to trigger the formation of fingers that desestablized into autonomous critters [13, 212, 213], see Fig.

8(c). In relatively diluted populations of colloidal rolling particles, HIs also leaded the appearance of coherent motion in the form of macroscopic 'flocks' or in that of a homogenous polar phase [69], see Fig. 3(a). In all the previous examples, propellers characterized by a small in-plane rotational diffusion, and persistent trajectories presented self-organization close to a surface. Spormann [214] and Carlile et al. [215] already reported that unidirectional magnetotactic bacteria swimming in cylindrical glass tubes and steered by an external magnetic field, formed stable bands that translated with their long axes perpendicular to their common direction of motion, as well as small lateral strings, consisting of as few as two or three cells. Band formation was also described in chemotactic bacteria [216], and these elongated structures were explained as resulting from HIs [203].

The hydrodynamic flow generated by a micro-object due to a chemical reaction induced by an external field, as a light source [217], not only can be used for producing self-propulsion, but also to induce long-range attractions that trigger particle assembly at the microscale. Even in systems composed by apolar particles [218], which can be externally activated but not show net propulsion [219], or in mixtures of active and passive colloids [126, 220], the presence of neighbouring particles leads to asymmetric electro-osmotic flows and consequently to long-range attractive interactions [218]. This results in the formation of active clusters, with controllable sizes and shapes as demonstrated in Ref. [220]. Such properties determine their translational and -rotational motions [221]. Systems comprised solely of motile active particles also display the formation of clustering [72], phase separation [68] or crystallization [222], depending on the particle constriction. In the dilute case, the formed clusters were found to easily break due to the delicate balance between self-propulsion and steric interactions between the interacting units [223]. For example, light activated colloid/hematite composites were found to propel and assemble under blue light due to the generated

osmotic flow. These "living crystals" were observed to dynamically break and reform, while displaying giant number fluctuations at high particle densities [224]. The combination of light activation with external magnetic field, was used as an efficient way for steering and propelling these nonequilibrium flow-induced assemblies [72, 126].

Hydrodynamic synchronization of interacting dynamical systems occurs when two autonomous system are able to move in unison, with a common frequency and a common phase, due to HIs [225, 226]. The time reversibility of the Stokes equations in principle do not allows synchronization, that is an irreversible process [12, 227]. However, time symmetry can be broken by using phase dependent torques [12] or by introducing some degree of mechanical flexibility in the actuated system [148, 228]. Important insights into physical mechanisms of hydrodynamic synchronization have been gained by the study of the synchronized behavior of flagella and cilia [11, 229]. Almost 100 years ago Gray observed that two nearby sperm cells synchronize the undulations of their flagella [230]. For more than 40 years there is experimental and theoretical evidence that the oscillating tails of nearby spermatozoa may synchronize due to their hydrodynamic coupling [34, 107]. However, only recently a clear experimental proof was obtained, by studying flagellated organisms held with micro-pipettes [231], see Fig 9(c). In those experiments, cilia deform in a non-reciprocal manner through the modulation of the driving force [30]. On the other hand, other mechanisms internal to the cell or based on the exchange of chemical signals could provide additional coupling, that is at the base of the flagellar coordination [229, 232, 233]. Due to hydrodynamic synchronization, carpets of cilia generate metachronal waves able to transport fluid, with a constant phase difference between two adjacent cilia [11, 186, 234-236]. Wollin et al., using a model system composed by a set of rowers placed on a periodic array and driven by an external non-linear force, showed

that HIs favor the emergence of metachronal waves only in the presence of a close surface [237]. Synchronization was also showed in arrays of artificial micro-actuators, and some of these actuated systems synchronized their oscillations through a weak coupling mediated by HIs [225]. For example, hydrodynamically coupled synchronization was noticed in "light-mill' micro-rotors finely driven by radiation pressure [227], see Fig. 9(d), and in colloids driven along circular or oscillatory trajectories, by using feedback-controlled optical tweezers [238, 239]. Here, synchronization was tuned through the modulation of the driving force and the deformability of the trajectory. In driven oscillating colloidal spheres, thermal noise established an upper limit on the distance between oscillators to maintain synchronization [239]. In another experiment shown in Fig. 9(e), different number of particles driven in rotating energy landscapes, created using holographic optical tweezers, rotated in phase led by the perturbations in the surrounding fluid [240]. The optical tweezers generated a sinusoidal energy landscape that was tilted due to the viscous drag exerted by the background flow on the driven particles. The degree of this inclination was determined by the relative phase of the neighboring particles. In this system, the local minima of the potential energy were deeper when the neighboring particles were synchronized. Since the synchronization of rotational or oscillatory motion may play an important role in swarming, the term "swarmalator" was proposed by O'Keeffe et al. to refer to those systems [241]. Swarming induced by the hydrodynamic synchronization was investigated in Ref. [242].

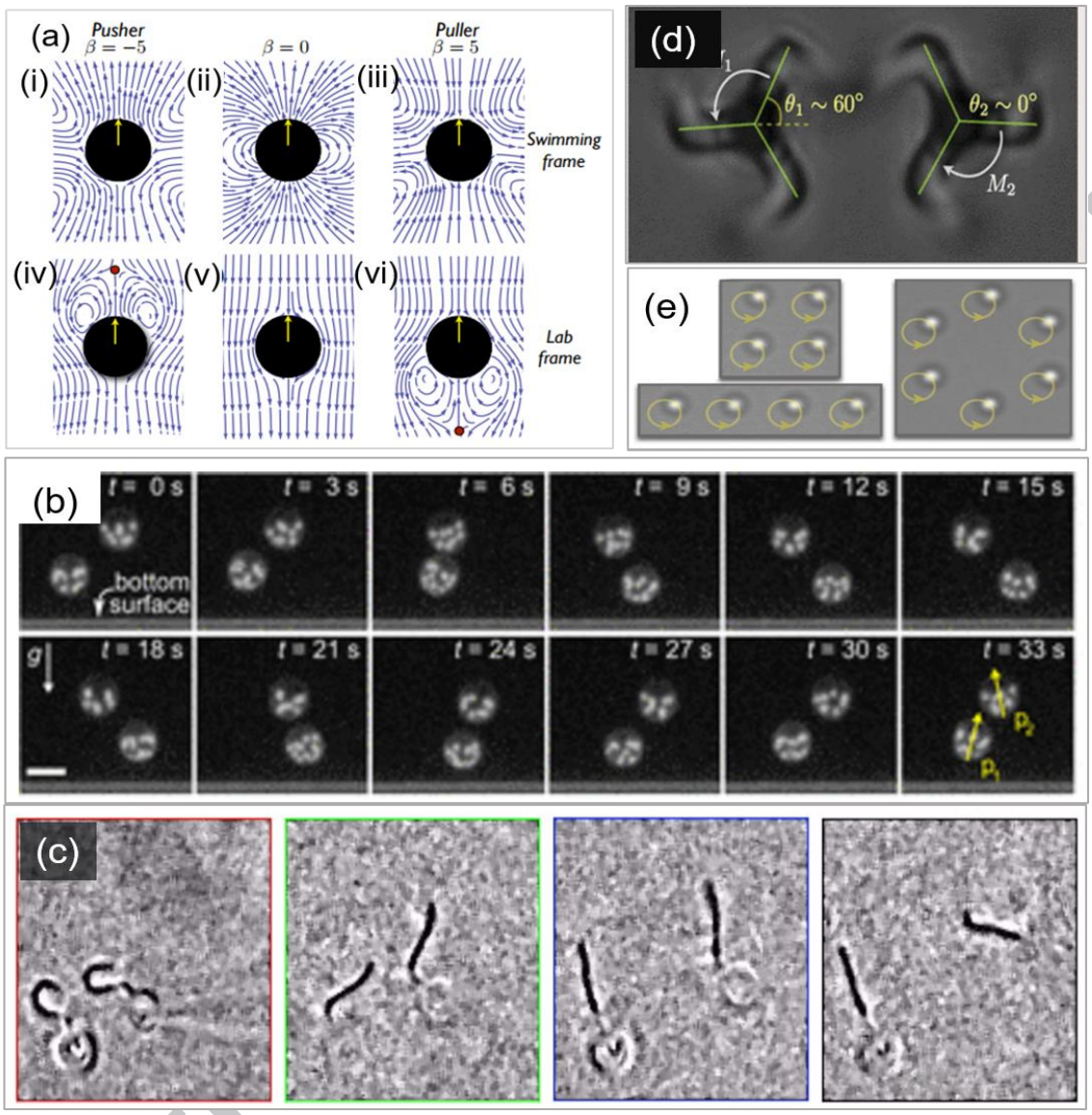

Fig. 9. (a) Flow streamlines of a pusher (first column), a neutral swimmer (central column) and a puller (last column), drawn in the swimming frame (top) and lab frame (bottom). The yellow arrows indicate the sense of motion. (b-e) Different bound and synchronous states favored by the HIs: (b) pairs of spinning dancing volvox in algae colonies orbit each other due to the interplay of short-range lubrication forces and solvent mediated forces. (c) Tails of nearby spermatozoa synchronize due to hydrodynamic coupling. (d) "Light-mill' micro-rotors driven by the radiation pressure of an incident laser beam, show temporal synchronize favored by HIs. (e) Different number of particles each placed in a rotating optical trap were synchronized via HIs. [(a) Reprinted with permission from Ref. [70] (Copyright 2011 AIP Publishing LLC), (b) Reprinted with permission from Ref. [211] (Copyright 2009 APS), (c) from Ref. [231] under the

Creative Commons 4.0 license, (d) from Ref. [227] (Copyright 2012 APS), and (e) from Ref. [240] (Copyright 2013 APS)].

7. Conclusions

In this article, we give an overview of recent works based on investigating the realization and dynamics of microscale propellers in presence of HIs. The development of new techniques to transport matter at low *Re* could also serve to control the fluids at the such scale, and understand how the flows generated by a set of micro-actuators, potentially rectified by the presence of external boundaries, interfere and operate. The different strategies reviewed here take advantage of using the fluid flow for swimming, transporting and inducing bound and synchronous states, without the need to establish irreversible chemical bonds, or to induce changes in the composition of the medium, factors that can be unfavorable when dealing with biological suspensions. Future challenges lie in using of more complex colloidal architectures, such as heterogeneous systems made up of particles with different geometrical, chemical, optical or magnetic features, capable of optimizing the load, transport and release of microcargos and drugs in biological environments. Further, such complex swimmers may have direct applications in vivo, or carrying out more complex tasks like chemical remediation, sorting, enhanced mixing, compressing, distorting or sieving. The design and implementation of hydrodynamic cooperative methods, with systems composed by many bound or synchronized actuators, may also help improving the capacity and efficiency of the previous applications. The strategies based on the individual manipulation of cargo, although impressive, are limited to specific actuations and to the requirement of continuous monitoring. Another future research direction may extend these techniques to different interfaces [243], where the hydrodynamic flows generated by the actuate particles may be used to trap or release particles from the interface, to

measure interfacial microrheological properties [244], or to influence on the stability of foams and emulsions [245, 246].

Acknowledgments

F.M.P. acknowledges support from MINECO (Grant No. RYC-2015-18495). P.T. acknowledges support from the ERC starting Grant "DynaMO" (No. 335040), from MINECO (FIS2016-78507-C2 AEI/FEDER-EU) and DURSI (2014SGR878).

References:

1. Grier, D.G., *A revolution in optical manipulation.* Nature, 2003. **424**(6950): p. 810-816.
2. Edwards, T.D. and M.A. Bevan, *Controlling Colloidal Particles with Electric Fields.* Langmuir, 2014. **30**(36): p. 10793-10803.
3. Erb, R.M. and B.B. Yellen, *Magnetic Manipulation of Colloidal Particles*, in *Nanoscale Magnetic Materials and Applications*, J.P. Liu, et al., Editors. 2009, Springer US: Boston, MA. p. 563-590.
4. Tierno, P., et al., *Magnetically Actuated Colloidal Microswimmers.* The Journal of Physical Chemistry B, 2008. **112**(51): p. 16525-16528.
5. Ebbens, S., *A fantastic voyage?* Materials Today, 2012. **15**(7): p. 294.
6. Lin, C.M., et al., *Trapping of Bioparticles via Microvortices in a Microfluidic Device for Bioassay Applications.* Analytical Chemistry, 2008. **80**(23): p. 8937-8945.
7. Lauga, E. and T.R. Powers, *The hydrodynamics of swimming microorganisms.* Reports on Progress in Physics, 2009. **72**(9): p. 096601.
8. Purcell, E.M., *Life at low Reynolds number.* American Journal of Physics, 1977. **45**(1): p. 3-11.
9. Lauga, E., *Bacterial Hydrodynamics.* Annual Review of Fluid Mechanics, 2016. **48**(1): p. 105-130.
10. Riedel, I.H., K. Kruse, and J. Howard, *A Self-Organized Vortex Array of Hydrodynamically Entrained Sperm Cells.* Science, 2005. **309**(5732): p. 300-303.
11. Brumley, D.R., et al., *Hydrodynamic Synchronization and Metachronal Waves on the Surface of the Colonial Alga Volvox carteri.* Physical Review Letters, 2012. **109**(26): p. 268102.
12. Uchida, N. and R. Golestanian, *Generic Conditions for Hydrodynamic Synchronization.* Physical Review Letters, 2011. **106**(5): p. 058104.
13. Driscoll, M., et al., *Unstable fronts and motile structures formed by microrollers.* Nat Phys, 2017. **13**(4): p. 375-379.
14. Martinez-Pedrero, F. and P. Tierno, *Magnetic Propulsion of Self-Assembled Colloidal Carpets: Efficient Cargo Transport via a Conveyor-Belt Effect.* Physical Review Applied, 2015. **3**(5): p. 6.
15. Happel, J. and H. Brenner, *Low Reynolds number hydrodynamics: with special applications to particulate media*. 1965: Prentice-Hall.
16. Dhont, J.K.G., *An Introduction to Dynamics of Colloids*. 1996: Elsevier Science.
17. Hinch, E.J., *Hydrodynamics at Low Reynolds Numbers: A Brief and Elementary Introduction*, in *Disorder and Mixing: Convection, Diffusion and Reaction in Random*

Materials and Processes, E. Guyon, J.-P. Nadal, and Y. Pomeau, Editors. 1988, Springer Netherlands: Dordrecht. p. 43-56.
18. Bechinger, C., F. Sciortino, and P. Ziherl, *Physics of Complex Colloids*. 2013: IOS Press.
19. *Microhydrodynamics*, S.J. Karrila, Editor. 1991, Butterworth-Heinemann.
20. Guazzelli, É., J.F. Morris, and S. Pic, *A Physical Introduction to Suspension Dynamics*. 2011: Cambridge University Press.
21. Lisicki, M., *Four approaches to hydrodynamic Green's functions -- the Oseen tensors.* 2013arXiv1312.6231L, 2013.
22. Jánosi, I.M., et al., *Chaotic particle dynamics in viscous flows: The three-particle Stokeslet problem.* Physical Review E, 1997. **56**(3): p. 2858-2868.
23. *Low Reynolds number flows*, G.I. Taylor and J. Friedman, Editors., Distributed by Encyclopaedia Britannica: [Chicago, Ill. :.
24. Stokes, G.G.S. and S. Cambridge Philosophical, *On the effect of the internal friction of fluids on the motion of pendulums*. 1851, Cambridge: printed at the Pitt Press, by John W. Parker, .. 99, [1] p. ; 29 cm.
25. Grier, D.G. and S.H. Behrens, *Interactions in Colloidal Suspensions*, in *Electrostatic Effects in Soft Matter and Biophysics: Proceedings of the NATO Advanced Research Workshop on Electrostatic Effects in Soft Matter and Biophysics Les Houches, France 1–13 October 2000*, C. Holm, P. Kékicheff, and R. Podgornik, Editors. 2001, Springer Netherlands: Dordrecht. p. 87-116.
26. Blake, J.R. and A.T. Chwang, *Fundamental singularities of viscous flow.* Journal of Engineering Mathematics, 1974. **8**(1): p. 23-29.
27. Brennen, C. and H. Winet, *Fluid Mechanics of Propulsion by Cilia and Flagella.* Annual Review of Fluid Mechanics, 1977. **9**(1): p. 339-398.
28. Martinez-Pedrero, F., et al., *Colloidal Microworms Propelling via a Cooperative Hydrodynamic Conveyor Belt.* Physical Review Letters, 2015. **115**(13): p. 138301.
29. Aragones, J.L., J.P. Steimel, and A. Alexander-Katz, *Elasticity-induced force reversal between active spinning particles in dense passive media.* 2016. **7**: p. 11325.
30. Eric, L. and R.P. Thomas, *The hydrodynamics of swimming microorganisms.* Reports on Progress in Physics, 2009. **72**(9): p. 096601.
31. Batchelor, G.K., *The stress system in a suspension of force-free particles.* Journal of Fluid Mechanics, 2006. **41**(3): p. 545-570.
32. Lisicki, M. and G. Nägele, *Colloidal Hydrodynamics and Interfacial Effects*, in *Soft Matter at Aqueous Interfaces*, P. Lang and Y. Liu, Editors. 2016, Springer International Publishing: Cham. p. 313-386.
33. Reichert, M., *Hydrodynamic Interactions in Colloidal and Biological Systems*. 2015: GRIN Publishing.
34. Taylor, G., *Analysis of the Swimming of Microscopic Organisms.* Proceedings of the Royal Society of London. Series A. Mathematical and Physical Sciences, 1951. **209**(1099): p. 447-461.
35. Trouilloud, R., et al., *Soft Swimming: Exploiting Deformable Interfaces for Low Reynolds Number Locomotion.* Physical Review Letters, 2008. **101**(4): p. 048102.
36. Diamant, H., et al., *Hydrodynamic interaction in quasi-two-dimensional suspensions.* Journal of Physics: Condensed Matter, 2005. **17**(31): p. S2787.
37. Goto, Y. and H. Tanaka, *Purely hydrodynamic ordering of rotating disks at a finite Reynolds number.* 2015. **6**: p. 5994.
38. Nägele, G. and P. Baur, *Influence of hydrodynamic interactions on long-time diffusion in charge-stabilized colloids.* Europhys. Lett., 1997. **38**(7): p. 557-562.
39. Härtl, W., et al., *Self-diffusion and hydrodynamic interactions in highly charged colloids.* Journal of Physics: Condensed Matter, 2000. **12**(8A): p. A287.

40. Zahn, K., J.M. Méndez-Alcaraz, and G. Maret, *Hydrodynamic Interactions May Enhance the Self-Diffusion of Colloidal Particles.* Physical Review Letters, 1997. **79**(1): p. 175-178.
41. Crocker, J.C., *Measurement of the hydrodynamic corrections to the Brownian motion of two colloidal spheres.* The Journal of Chemical Physics, 1997. **106**(7): p. 2837-2840.
42. Meiners, J.-C. and S.R. Quake, *Direct Measurement of Hydrodynamic Cross Correlations between Two Particles in an External Potential.* Physical Review Letters, 1999. **82**(10): p. 2211-2214.
43. Adamczyk, Z., *Series Editors*, in *Interface Science and Technology*, Z. Adamczyk, Editor. 2006, Elsevier. p. ii.
44. Li, S., H. Jiang, and Z. Hou, *Effects of hydrodynamic interactions on the crystallization of passive and active colloidal systems.* Soft Matter, 2015. **11**(28): p. 5712-5718.
45. Schilling, T., et al., *Crystallization in suspensions of hard spheres: a Monte Carlo and molecular dynamics simulation study.* Journal of Physics: Condensed Matter, 2011. **23**(19): p. 194120.
46. Radu, M. and T. Schilling, *Solvent hydrodynamics speed up crystal nucleation in suspensions of hard spheres.* EPL (Europhysics Letters), 2014. **105**(2): p. 26001.
47. Roehm, D., S. Kesselheim, and A. Arnold, *Hydrodynamic interactions slow down crystallization of soft colloids.* Soft Matter, 2014. **10**(30): p. 5503-5509.
48. Groot, R.D., T.J. Madden, and D.J. Tildesley, *On the role of hydrodynamic interactions in block copolymer microphase separation.* The Journal of Chemical Physics, 1999. **110**(19): p. 9739-9749.
49. Beatus, T., et al., *Two-dimensional flow of driven particles: a microfluidic pathway to the non-equilibrium frontier.* Chemical Society Reviews, 2017. **46**(18): p. 5620-5646.
50. Lutz, C., et al., *Surmounting barriers: The benefit of hydrodynamic interactions.* EPL (Europhysics Letters), 2006. **74**(4): p. 719.
51. Squires, T.M. and M.P. Brenner, *Like-Charge Attraction and Hydrodynamic Interaction.* Physical Review Letters, 2000. **85**(23): p. 4976-4979.
52. Sokolov, Y., et al., *Hydrodynamic Pair Attractions between Driven Colloidal Particles.* Physical Review Letters, 2011. **107**(15): p. 158302.
53. Roichman, Y., D.G. Grier, and G. Zaslavsky, *Anomalous collective dynamics in optically driven colloidal rings.* Physical Review E, 2007. **75**(2): p. 020401.
54. Erb, R.M., et al., *Actuating Soft Matter with Magnetic Torque.* Advanced Functional Materials, 2016. **26**(22): p. 3859-3880.
55. Sawetzki, T., et al., *In situ assembly of linked geometrically coupled microdevices.* Proceedings of the National Academy of Sciences, 2008. **105**(51): p. 20141-20145.
56. Shlomovitz, R., et al., *Probing interfacial dynamics and mechanics using submerged particle microrheology. I. Theory.* Physics of Fluids, 2014. **26**(7): p. 071903.
57. Boatwright, T., et al., *Probing interfacial dynamics and mechanics using submerged particle microrheology. II. Experiment.* Physics of Fluids, 2014. **26**(7): p. 071904.
58. Hajime, T., *Roles of hydrodynamic interactions in structure formation of soft matter: protein folding as an example.* Journal of Physics: Condensed Matter, 2005. **17**(31): p. S2795.
59. Piotr, S. and C. Marek, *Hydrodynamic effects in proteins.* Journal of Physics: Condensed Matter, 2011. **23**(3): p. 033102.
60. Brune, D. and S. Kim, *Hydrodynamic steering effects in protein association.* Proceedings of the National Academy of Sciences of the United States of America, 1994. **91**(8): p. 2930-2934.
61. Batchelor, G.K., *Sedimentation in a dilute dispersion of spheres.* Journal of Fluid Mechanics, 2006. **52**(2): p. 245-268.
62. Caflisch, R.E. and J.H.C. Luke, *Variance in the sedimentation speed of a suspension.* The Physics of Fluids, 1985. **28**(3): p. 759-760.

63. Segrè, P.N., E. Herbolzheimer, and P.M. Chaikin, *Long-Range Correlations in Sedimentation.* Physical Review Letters, 1997. **79**(13): p. 2574-2577.
64. Segre, P.N., et al., *An effective gravitational temperature for sedimentation.* Nature, 2001. **409**(6820): p. 594-597.
65. Tee, S.-Y., et al., *Nonuniversal Velocity Fluctuations of Sedimenting Particles.* Physical Review Letters, 2002. **89**(5): p. 054501.
66. Gómez, D.C., et al., *On stratification control of the velocity fluctuations in sedimentation.* Physics of Fluids, 2007. **19**(9): p. 098102.
67. Möller, J. and T. Narayanan, *Velocity Fluctuations in Sedimenting Brownian Particles.* Physical Review Letters, 2017. **118**(19): p. 198001.
68. Zöttl, A. and H. Stark, *Hydrodynamics Determines Collective Motion and Phase Behavior of Active Colloids in Quasi-Two-Dimensional Confinement.* Physical Review Letters, 2014. **112**(11): p. 118101.
69. Bricard, A., et al., *Emergence of macroscopic directed motion in populations of motile colloids.* Nature, 2013. **503**(7474): p. 95-98.
70. Evans, A.A., et al., *Orientational order in concentrated suspensions of spherical microswimmers.* Physics of Fluids, 2011. **23**(11): p. 111702.
71. Matas-Navarro, R., et al., *Hydrodynamic suppression of phase separation in active suspensions.* Physical Review E, 2014. **90**(3): p. 032304.
72. Palacci, J., et al., *Living Crystals of Light-Activated Colloidal Surfers.* Science, 2013. **339**(6122): p. 936-940.
73. Buttinoni, I., et al., *Dynamical Clustering and Phase Separation in Suspensions of Self-Propelled Colloidal Particles.* Physical Review Letters, 2013. **110**(23): p. 238301.
74. Gonnella, G., et al., *Motility-induced phase separation and coarsening in active matter.* Comptes Rendus Physique, 2015. **16**(3): p. 316-331.
75. Furukawa, A. and H. Tanaka, *Key Role of Hydrodynamic Interactions in Colloidal Gelation.* Physical Review Letters, 2010. **104**(24): p. 245702.
76. Varga, Z. and J. Swan, *Hydrodynamic interactions enhance gelation in dispersions of colloids with short-ranged attraction and long-ranged repulsion.* Soft Matter, 2016. **12**(36): p. 7670-7681.
77. Ando, T. and J. Skolnick, *Sliding of Proteins Non-specifically Bound to DNA: Brownian Dynamics Studies with Coarse-Grained Protein and DNA Models.* PLOS Computational Biology, 2014. **10**(12): p. e1003990.
78. Roosen-Runge, F., et al., *Protein self-diffusion in crowded solutions.* Proceedings of the National Academy of Sciences, 2011. **108**(29): p. 11815-11820.
79. Riedel-Kruse, I.H., et al., *How molecular motors shape the flagellar beat.* HFSP Journal, 2007. **1**(3): p. 192-208.
80. Goldtzvik, Y., Z. Zhang, and D. Thirumalai, *Importance of Hydrodynamic Interactions in the Stepping Kinetics of Kinesin.* The Journal of Physical Chemistry B, 2016. **120**(8): p. 2071-2075.
81. Skolnick, J., *Perspective: On the importance of hydrodynamic interactions in the subcellular dynamics of macromolecules.* The Journal of Chemical Physics, 2016. **145**(10): p. 100901.
82. Ando, T. and J. Skolnick, *On the Importance of Hydrodynamic Interactions in Lipid Membrane Formation.* Biophysical Journal, 2013. **104**(1): p. 96-105.
83. Woodhouse, F.G. and R.E. Goldstein, *Cytoplasmic streaming in plant cells emerges naturally by microfilament self-organization.* Proceedings of the National Academy of Sciences, 2013. **110**(35): p. 14132-14137.
84. Peyer, K.E., L. Zhang, and B.J. Nelson, *Bio-inspired magnetic swimming microrobots for biomedical applications.* Nanoscale, 2013. **5**(4): p. 1259-1272.
85. Nelson, B.J., I.K. Kaliakatsos, and J.J. Abbott, *Microrobots for Minimally Invasive Medicine.* Annual Review of Biomedical Engineering, 2010. **12**(1): p. 55-85.

86. Wang, J., *Cargo-towing synthetic nanomachines: Towards active transport in microchip devices.* Lab on a Chip, 2012. **12**(11): p. 1944-1950.
87. Sanchez, S., et al., *Microbots Swimming in the Flowing Streams of Microfluidic Channels.* Journal of the American Chemical Society, 2011. **133**(4): p. 701-703.
88. Golestanian, R. and A. Ajdari, *Analytic results for the three-sphere swimmer at low Reynolds number.* Physical Review E, 2008. **77**(3): p. 036308.
89. Lauga, E. and D. Bartolo, *No many-scallop theorem: Collective locomotion of reciprocal swimmers.* Physical Review E, 2008. **78**(3): p. 030901.
90. Sanchez, S., et al., *Superfast Motion of Catalytic Microjet Engines at Physiological Temperature.* Journal of the American Chemical Society, 2011. **133**(38): p. 14860-14863.
91. Wang, W., et al., *Autonomous Motion of Metallic Microrods Propelled by Ultrasound.* ACS Nano, 2012. **6**(7): p. 6122-6132.
92. Jiang, H.-R., N. Yoshinaga, and M. Sano, *Active Motion of a Janus Particle by Self-Thermophoresis in a Defocused Laser Beam.* Physical Review Letters, 2010. **105**(26): p. 268302.
93. Celedon, A., Christopher M. Hale, and D. Wirtz, *Magnetic Manipulation of Nanorods in the Nucleus of Living Cells.* Biophysical Journal, 2011. **101**(8): p. 1880-1886.
94. Pamme, N., *Magnetism and microfluidics.* Lab on a Chip, 2006. **6**(1): p. 24-38.
95. Abbott, J.J., et al., *How Should Microrobots Swim?* The International Journal of Robotics Research, 2009. **28**(11-12): p. 1434-1447.
96. Fournier-Bidoz, S., et al., *Synthetic self-propelled nanorotors.* Chemical Communications, 2005(4): p. 441-443.
97. Mano, N. and A. Heller, *Bioelectrochemical Propulsion.* Journal of the American Chemical Society, 2005. **127**(33): p. 11574-11575.
98. Howse, J.R., et al., *Self-Motile Colloidal Particles: From Directed Propulsion to Random Walk.* Physical Review Letters, 2007. **99**(4): p. 048102.
99. Michelin, S. and E. Lauga, *Geometric tuning of self-propulsion for Janus catalytic particles.* Scientific Reports, 2017. **7**: p. 42264.
100. Paxton, W.F., et al., *Catalytic Nanomotors: Autonomous Movement of Striped Nanorods.* Journal of the American Chemical Society, 2004. **126**(41): p. 13424-13431.
101. Ebbens, S.J., *Active colloids: Progress and challenges towards realising autonomous applications.* Current Opinion in Colloid & Interface Science, 2016. **21**(Supplement C): p. 14-23.
102. Bell, D.J., et al. *Flagella-like Propulsion for Microrobots Using a Nanocoil and a Rotating Electromagnetic Field*. in *Proceedings 2007 IEEE International Conference on Robotics and Automation*. 2007.
103. Tottori, S., et al., *Magnetic Helical Micromachines: Fabrication, Controlled Swimming, and Cargo Transport.* Advanced Materials, 2012. **24**(6): p. 811-816.
104. Ghosh, A. and P. Fischer, *Controlled Propulsion of Artificial Magnetic Nanostructured Propellers.* Nano Letters, 2009. **9**(6): p. 2243-2245.
105. Honda, T., K.I. Arai, and K. Ishiyama, *Micro swimming mechanisms propelled by external magnetic fields.* IEEE Transactions on Magnetics, 1996. **32**(5): p. 5085-5087.
106. Mandal, P. and A. Ghosh, *Observation of Enhanced Diffusivity in Magnetically Powered Reciprocal Swimmers.* Physical Review Letters, 2013. **111**(24): p. 248101.
107. Berg, H.C. and R.A. Anderson, *Bacteria Swim by Rotating their Flagellar Filaments.* Nature, 1973. **245**(5425): p. 380-382.
108. Spagnolie, S.E. and E. Lauga, *Comparative Hydrodynamics of Bacterial Polymorphism.* Physical Review Letters, 2011. **106**(5): p. 058103.
109. Turner, L., W.S. Ryu, and H.C. Berg, *Real-Time Imaging of Fluorescent Flagellar Filaments.* Journal of Bacteriology, 2000. **182**(10): p. 2793-2801.

110. S C Schuster, a. and S. Khan, *The Bacterial Flagellar Motor.* Annual Review of Biophysics and Biomolecular Structure, 1994. **23**(1): p. 509-539.
111. Kim, M., et al., *A macroscopic scale model of bacterial flagellar bundling.* Proceedings of the National Academy of Sciences, 2003. **100**(26): p. 15481-15485.
112. Xu, T., et al., *Influence of geometry on swimming performance of helical swimmers using DoE.* Journal of Micro-Bio Robotics, 2016. **11**(1): p. 57-66.
113. Cheang, U.K., et al., *Minimal geometric requirements for micropropulsion via magnetic rotation.* Physical Review E, 2014. **90**(3): p. 033007.
114. Morozov, K.I., et al., *Dynamics of arbitrary shaped propellers driven by a rotating magnetic field.* Physical Review Fluids, 2017. **2**(4): p. 044202.
115. Keaveny, E.E., S.W. Walker, and M.J. Shelley, *Optimization of Chiral Structures for Microscale Propulsion.* Nano Letters, 2013. **13**(2): p. 531-537.
116. Wan, M.B., et al., *Rectification of Swimming Bacteria and Self-Driven Particle Systems by Arrays of Asymmetric Barriers.* Physical Review Letters, 2008. **101**(1): p. 018102.
117. Berke, A.P., et al., *Hydrodynamic Attraction of Swimming Microorganisms by Surfaces.* Physical Review Letters, 2008. **101**(3): p. 038102.
118. Lauga, E., et al., *Swimming in Circles: Motion of Bacteria near Solid Boundaries.* Biophysical Journal, 2006. **90**(2): p. 400-412.
119. Goldman, A.J., R.G. Cox, and H. Brenner, *Slow viscous motion of a sphere parallel to a plane wall—I Motion through a quiescent fluid.* Chemical Engineering Science, 1967. **22**(4): p. 637-651.
120. Blake, J.R., *A note on the image system for a stokeslet in a no-slip boundary.* Mathematical Proceedings of the Cambridge Philosophical Society, 2008. **70**(2): p. 303-310.
121. Jeffrey, D.J. and Y. Onishi, *The Slow Sotion of a Cylinder Next to Plane Wall.* The Quarterly Journal of Mechanics and Applied Mathematics, 1981. **34**(2): p. 129-137.
122. Casic, N., et al., *Propulsion Efficiency of a Dynamic Self-Assembled Helical Ribbon.* Physical Review Letters, 2013. **110**(16): p. 4.
123. Tierno, P., R. Muruganathan, and T.M. Fischer, *Viscoelasticity of Dynamically Self-Assembled Paramagnetic Colloidal Clusters.* Physical Review Letters, 2007. **98**(2): p. 028301.
124. Janssen, X.J.A., et al., *Controlled torque on superparamagnetic beads for functional biosensors.* Biosensors and Bioelectronics, 2009. **24**(7): p. 1937-1941.
125. Nathan J. Jenness, et al., *Magnetic and optical manipulation of spherical metal-coated Janus particles.* Optical Trapping and Optical Micromanipulation VII, 2010. **7762**(776227).
126. Martinez-Pedrero, F., H. Massana-Cid, and P. Tierno, *Assembly and Transport of Microscopic Cargos via Reconfigurable Photoactivated Magnetic Microdockers.* Small, 2017. **13**(18): p. 1603449-n/a.
127. Zhang, L., et al., *Controlled Propulsion and Cargo Transport of Rotating Nickel Nanowires near a Patterned Solid Surface.* ACS Nano, 2010. **4**(10): p. 6228-6234.
128. Tierno, P., et al., *Controlled Swimming in Confined Fluids of Magnetically Actuated Colloidal Rotors.* Physical Review Letters, 2008. **101**(21): p. 218304.
129. Tierno, P., et al., *Controlled propulsion in viscous fluids of magnetically actuated colloidal doublets.* Physical Review E, 2010. **81**(1): p. 011402.
130. Sing, C.E., et al., *Controlled surface-induced flows from the motion of self-assembled colloidal walkers.* Proceedings of the National Academy of Sciences, 2010. **107**(2): p. 535-540.
131. Di Leonardo, R., et al., *Swimming with an Image.* Physical Review Letters, 2011. **106**(3): p. 038101.
132. Massana-Cid, H., et al., *Propulsion and hydrodynamic particle transport of magnetically twisted colloidal ribbons.* New Journal of Physics, 2017.

133. Martinez-Pedrero, F., A. Cebers, and P. Tierno, *Orientational dynamics of colloidal ribbons self-assembled from microscopic magnetic ellipsoids.* Soft Matter, 2016. **12**(16): p. 3688-3695.
134. Götze, I.O. and G. Gompper, *Flow generation by rotating colloids in planar microchannels.* EPL (Europhysics Letters), 2010. **92**(6): p. 64003.
135. Tirado, M.M. and J.G. de la Torre, *Rotational dynamics of rigid, symmetric top macromolecules. Application to circular cylinders.* The Journal of Chemical Physics, 1980. **73**(4): p. 1986-1993.
136. Manghi, M., et al., *Hydrodynamic effects in driven soft matter.* Soft Matter, 2006. **2**(8): p. 653-668.
137. Pak, O.S. and E. Lauga, *CHAPTER 4 Theoretical Models of Low-Reynolds-Number Locomotion*, in *Fluid-Structure Interactions in Low-Reynolds-Number Flows*. 2016, The Royal Society of Chemistry. p. 100-167.
138. Chwang, A.T. and T.Y. Wu, *A note on the helical movement of micro-organisms.* Proceedings of the Royal Society of London. Series B. Biological Sciences, 1971. **178**(1052): p. 327.
139. Peng, Z., G.J. Elfring, and O.S. Pak, *Maximizing propulsive thrust of a driven filament at low Reynolds number via variable flexibility.* Soft Matter, 2017. **13**(12): p. 2339-2347.
140. GRAY, J. and G.J. HANCOCK, *The Propulsion of Sea-Urchin Spermatozoa.* Journal of Experimental Biology, 1955. **32**(4): p. 802-814.
141. Higdon, J.J.L., *A hydrodynamic analysis of flagellar propulsion.* Journal of Fluid Mechanics, 1979. **90**(4): p. 685-711.
142. Lighthill, J., *Flagellar Hydrodynamics.* SIAM Review, 1976. **18**(2): p. 161-230.
143. Kim, M. and T.R. Powers, *Deformation of a helical filament by flow and electric or magnetic fields.* Physical Review E, 2005. **71**(2): p. 021914.
144. Jawed, M.K., et al., *Propulsion and Instability of a Flexible Helical Rod Rotating in a Viscous Fluid.* Physical Review Letters, 2015. **115**(16): p. 168101.
145. Takano, Y., et al., *Analysis of Small Deformation of Helical Flagellum of Swimming Vibrio alginolyticus.* JSME International Journal Series C Mechanical Systems, Machine Elements and Manufacturing, 2003. **46**(4): p. 1241-1247.
146. Olson, S.D., S. Lim, and R. Cortez, *Modeling the dynamics of an elastic rod with intrinsic curvature and twist using a regularized Stokes formulation.* Journal of Computational Physics, 2013. **238**: p. 169-187.
147. Bergou, M., et al., *Discrete viscous threads.* ACM Trans. Graph., 2010. **29**(4): p. 1-10.
148. Vilfan, A. and F. Jülicher, *Hydrodynamic Flow Patterns and Synchronization of Beating Cilia.* Physical Review Letters, 2006. **96**(5): p. 058102.
149. Dreyfus, R., et al., *Microscopic artificial swimmers.* Nature, 2005. **437**(7060): p. 862-865.
150. Roper, M., et al., *Do magnetic micro-swimmers move like eukaryotic cells?* Proceedings of the Royal Society A: Mathematical, Physical and Engineering Science, 2008. **464**(2092): p. 877.
151. Gao, W., et al., *Magnetically Powered Flexible Metal Nanowire Motors.* Journal of the American Chemical Society, 2010. **132**(41): p. 14403-14405.
152. Pak, O.S., et al., *High-speed propulsion of flexible nanowire motors: Theory and experiments.* Soft Matter, 2011. **7**(18): p. 8169-8181.
153. Thomases, B. and R.D. Guy, *The role of body flexibility in stroke enhancements for finite-length undulatory swimmers in viscoelastic fluids.* Journal of Fluid Mechanics, 2017. **825**: p. 109-132.
154. Qiu, T., et al., *Swimming by reciprocal motion at low Reynolds number.* Nature Communications, 2014. **5**: p. 5119.
155. Dias, M.A. and T.R. Powers, *Swimming near deformable membranes at low Reynolds number.* Physics of Fluids, 2013. **25**(10): p. 101901.

156. Palacci, J., et al., *Photoactivated Colloidal Dockers for Cargo Transportation.* Journal of the American Chemical Society, 2013. **135**(43): p. 15978-15981.
157. Sanchez, S., et al., *Controlled manipulation of multiple cells using catalytic microbots.* Chemical Communications, 2011. **47**(2): p. 698-700.
158. Sundararajan, S., et al., *Catalytic Motors for Transport of Colloidal Cargo.* Nano Letters, 2008. **8**(5): p. 1271-1276.
159. Solovev, A.A., et al., *Magnetic Control of Tubular Catalytic Microbots for the Transport, Assembly, and Delivery of Micro-objects.* Advanced Functional Materials, 2010. **20**(15): p. 2430-2435.
160. Baraban, L., et al., *Catalytic Janus Motors on Microfluidic Chip: Deterministic Motion for Targeted Cargo Delivery.* ACS Nano, 2012. **6**(4): p. 3383-3389.
161. Fan, D., et al., *Subcellular-resolution delivery of a cytokine through precisely manipulated nanowires.* Nat Nano, 2010. **5**(7): p. 545-551.
162. Ashkin, A., et al., *Observation of a single-beam gradient force optical trap for dielectric particles.* Optics Letters, 1986. **11**(5): p. 288-290.
163. Hernandez-Navarro, S., et al., *Nematic Colloidal Swarms Assembled and Transported on Photosensitive Surfaces.* Ieee Transactions on Nanobioscience, 2015. **14**(3): p. 267-271.
164. Weibel, D.B., et al., *Microoxen: Microorganisms to move microscale loads.* Proceedings of the National Academy of Sciences of the United States of America, 2005. **102**(34): p. 11963-11967.
165. Ding, X., et al., *Standing surface acoustic wave (SSAW) based multichannel cell sorting.* Lab on a chip, 2012. **12**(21): p. 4228-4231.
166. Cai, D., et al., *Highly efficient molecular delivery into mammalian cells using carbon nanotube spearing.* Nat Meth, 2005. **2**(6): p. 449-454.
167. Gosse, C. and V. Croquette, *Magnetic Tweezers: Micromanipulation and Force Measurement at the Molecular Level.* Biophysical Journal, 2002. **82**(6): p. 3314-3329.
168. Tierno, P., et al., *Transport of Loaded and Unloaded Microcarriers in a Colloidal Magnetic Shift Register.* The Journal of Physical Chemistry B, 2007. **111**(48): p. 13479-13482.
169. Martinez-Pedrero, F., et al., *Functional colloidal micro-sieves assembled and guided above a channel-free magnetic striped film.* Lab on a Chip, 2015. **15**(7): p. 1765-1771.
170. Konrad, J.B., et al., *Motor protein-driven unidirectional transport of micrometer-sized cargoes across isopolar microtubule arrays.* Nanotechnology, 2001. **12**(3): p. 238.
171. Shelby, J.P. and D.T. Chiu, *Controlled rotation of biological micro- and nano-particles in microvortices.* Lab on a Chip, 2004. **4**(3): p. 168-170.
172. Shelby, J.P., S.A. Mutch, and D.T. Chiu, *Direct Manipulation and Observation of the Rotational Motion of Single Optically Trapped Microparticles and Biological Cells in Microvortices.* Analytical Chemistry, 2004. **76**(9): p. 2492-2497.
173. Karimi, A., S. Yazdi, and A.M. Ardekani, *Hydrodynamic mechanisms of cell and particle trapping in microfluidics.* Biomicrofluidics, 2013. **7**(2): p. 021501.
174. Wang, C., S.V. Jalikop, and S. Hilgenfeldt, *Efficient manipulation of microparticles in bubble streaming flows.* Biomicrofluidics, 2012. **6**(1): p. 012801.
175. Yazdi, S. and A.M. Ardekani, *Bacterial aggregation and biofilm formation in a vortical flow.* Biomicrofluidics, 2012. **6**(4): p. 044114.
176. Kajorndejnukul, V., S. Sukhov, and A. Dogariu, *Efficient mass transport by optical advection.* 2015. **5**: p. 14861.
177. Gauger, E.M., M.T. Downton, and H. Stark, *Fluid transport at low Reynolds number with magnetically actuated artificial cilia.* The European Physical Journal E, 2009. **28**(2): p. 231-242.
178. Vilfan, M., et al., *Self-assembled artificial cilia.* Proceedings of the National Academy of Sciences, 2010. **107**(5): p. 1844-1847.

179. Petit, T., et al., *Selective Trapping and Manipulation of Microscale Objects Using Mobile Microvortices.* Nano Letters, 2012. **12**(1): p. 156-160.
180. Maier, F.J. and T.M. Fischer, *Transport on Active Paramagnetic Colloidal Networks.* The Journal of Physical Chemistry B, 2016. **120**(38): p. 10162-10165.
181. Martinez-Pedrero, F., A. Cebers, and P. Tierno, *Dipolar Rings of Microscopic Ellipsoids: Magnetic Manipulation and Cell Entrapment.* Physical Review Applied, 2016. **6**(3): p. 034002.
182. Yang, T., et al., *Magnetic Microlassos for Reversible Cargo Capture, Transport, and Release.* Langmuir, 2017. **33**(23): p. 5932-5937.
183. Sakar, M.S., et al., *Single cell manipulation using ferromagnetic composite microtransporters.* Applied Physics Letters, 2010. **96**(4): p. 043705.
184. Khuc Trong, P., J. Guck, and R.E. Goldstein, *Coupling of Active Motion and Advection Shapes Intracellular Cargo Transport.* Physical Review Letters, 2012. **109**(2): p. 028104.
185. Shimmen, T., *The sliding theory of cytoplasmic streaming: fifty years of progress.* Journal of Plant Research, 2007. **120**(1): p. 31-43.
186. Elgeti, J. and G. Gompper, *Emergence of metachronal waves in cilia arrays.* Proceedings of the National Academy of Sciences, 2013. **110**(12): p. 4470-4475.
187. Manna, R.K., P.B.S. Kumar, and R. Adhikari, *Colloidal transport by active filaments.* The Journal of Chemical Physics, 2017. **146**(2): p. 024901.
188. Martin, S., et al., *Direct Observation of Hydrodynamic Rotation-Translation Coupling between Two Colloidal Spheres.* Physical Review Letters, 2006. **97**(24): p. 248301.
189. Reichert, M. and H. Stark, *Hydrodynamic coupling of two rotating spheres trapped in harmonic potentials.* Physical Review E, 2004. **69**(3): p. 031407.
190. Snook, I.K., K.M. Briggs, and E.R. Smith, *Hydrodynamic interactions and some new periodic structures in three particle sediments.* Physica A: Statistical Mechanics and its Applications, 1997. **240**(3): p. 547-559.
191. Nagar, H. and Y. Roichman, *Collective excitations of hydrodynamically coupled driven colloidal particles.* Physical Review E, 2014. **90**(4): p. 042302.
192. Leoni, M. and T.B. Liverpool, *Dynamics and interactions of active rotors.* EPL (Europhysics Letters), 2010. **92**(6): p. 64004.
193. Lenz, P., et al., *Membranes with rotating motors: Microvortex assemblies.* The European Physical Journal E, 2004. **13**(4): p. 379-390.
194. Grzybowski, B.A., H.A. Stone, and G.M. Whitesides, *Dynamic self-assembly of magnetized, millimetre-sized objects rotating at a liquid-air interface.* Nature, 2000. **405**(6790): p. 1033-1036.
195. Uspal, W.E. and P.S. Doyle, *Self-organizing microfluidic crystals.* Soft Matter, 2014. **10**(28): p. 5177-5191.
196. Lee, W., et al., *Dynamic self-assembly and control of microfluidic particle crystals.* Proceedings of the National Academy of Sciences of the United States of America, 2010. **107**(52): p. 22413-22418.
197. Koch, D.L. and G. Subramanian, *Collective Hydrodynamics of Swimming Microorganisms: Living Fluids.* Annual Review of Fluid Mechanics, 2011. **43**(1): p. 637-659.
198. Sokolov, A., et al., *Concentration Dependence of the Collective Dynamics of Swimming Bacteria.* Physical Review Letters, 2007. **98**(15): p. 158102.
199. Moore, H., et al., *Exceptional sperm cooperation in the wood mouse.* Nature, 2002. **418**(6894): p. 174-177.
200. Lighthill, M.J., *On the squirming motion of nearly spherical deformable bodies through liquids at very small {R}eynolds numbers.* Communications on Pure and Applied Mathematics, 1952. **5**: p. 109-118.
201. Blake, J.R., *A spherical envelope approach to ciliary propulsion.* Journal of Fluid Mechanics, 1971. **46**(1): p. 199-208.

202. Chisholm, N.G., et al., *A squirmer across Reynolds numbers.* Journal of Fluid Mechanics, 2016. **796**: p. 233-256.
203. Guell, D.C., et al., *Hydrodynamic forces and band formation in swimming magnetotactic bacteria.* Journal of Theoretical Biology, 1988. **135**(4): p. 525-542.
204. Ishikawa, T., et al., *Hydrodynamic Interactions between Two Swimming Bacteria.* Biophysical Journal, 2007. **93**(6): p. 2217-2225.
205. Guzmán-Lastra, F., A. Kaiser, and H. Löwen, *Fission and fusion scenarios for magnetic microswimmer clusters.* 2016. **7**: p. 13519.
206. Alarcón, F. and I. Pagonabarraga, *Spontaneous aggregation and global polar ordering in squirmer suspensions.* Journal of Molecular Liquids, 2013. **185**(Supplement C): p. 56-61.
207. Shashi, T., S. Ralf, and H. Stephan, *Swarming behavior of simple model squirmers.* New Journal of Physics, 2011. **13**(7): p. 073021.
208. Ishikawa, T. and T.J. Pedley, *Coherent Structures in Monolayers of Swimming Particles.* Physical Review Letters, 2008. **100**(8): p. 088103.
209. Delfau, J.-B., J. Molina, and M. Sano, *Collective behavior of strongly confined suspensions of squirmers.* EPL, 2016. **114**(2): p. 24001.
210. Dufresne, E.R., et al., *Hydrodynamic Coupling of Two Brownian Spheres to a Planar Surface.* Physical Review Letters, 2000. **85**(15): p. 3317-3320.
211. Drescher, K., et al., *Dancing Volvox: Hydrodynamic Bound States of Swimming Algae.* Physical review letters, 2009. **102**(16): p. 168101-168101.
212. Martinez-Pedrero, F., et al., *Emergent Hydrodynamic Bound States Between Magnetically Powered Micropropellers.* arXiv:1709.04229 [cond-mat.soft], 2017.
213. Tierno, P., *Colloids: A microscopic army.* Nat Phys, 2017. **13**(4): p. 324-326.
214. Spormann, A.M., *Unusual swimming behavior of a magnetotactic bacterium.* FEMS Microbiology Ecology, 1987. **3**(1): p. 37-45.
215. Carlile, M.J., et al., *Zoned migration of magnetotactic bacteria.* Journal of Magnetism and Magnetic Materials, 1987. **67**(3): p. 291-294.
216. Adler, J., *Chemotaxis in Bacteria.* Science, 1966. **153**(3737): p. 708-716.
217. Guix, M., et al., *Self-Propelled Micro/Nanoparticle Motors.* Particle & Particle Systems Characterization: p. 1700382-n/a.
218. Niu, R., T. Palberg, and T. Speck, *Self-Assembly of Colloidal Molecules due to Self-Generated Flow.* Physical Review Letters, 2017. **119**(2): p. 028001.
219. Davies Wykes, M.S., et al., *Dynamic self-assembly of microscale rotors and swimmers.* Soft Matter, 2016. **12**(20): p. 4584-4589.
220. Singh, D.P., et al., *Non-Equilibrium Assembly of Light-Activated Colloidal Mixtures.* Advanced Materials, 2017. **29**(32): p. 1701328-n/a.
221. Schmidt F., et al., *Light-controlled Assembly of Active Colloidal Molecules.* arXiv:1801.06868v1, 2018.
222. Bialké, J., T. Speck, and H. Löwen, *Crystallization in a Dense Suspension of Self-Propelled Particles.* Physical Review Letters, 2012. **108**(16): p. 168301.
223. Bechinger, C., et al., *Active particles in complex and crowded environments.* Reviews of Modern Physics, 2016. **88**(4): p. 045006.
224. Narayan, V., S. Ramaswamy, and N. Menon, *Long-Lived Giant Number Fluctuations in a Swarming Granular Nematic.* Science, 2007. **317**(5834): p. 105.
225. Friedrich, B., *Hydrodynamic synchronization of flagellar oscillators.* The European Physical Journal Special Topics, 2016. **225**(11): p. 2353-2368.
226. Golestanian, R., J.M. Yeomans, and N. Uchida, *Hydrodynamic synchronization at low Reynolds number.* Soft Matter, 2011. **7**(7): p. 3074-3082.
227. Di Leonardo, R., et al., *Hydrodynamic Synchronization of Light Driven Microrotors.* Physical Review Letters, 2012. **109**(3): p. 034104.

228. Reichert, M. and H. Stark, *Synchronization of rotating helices by hydrodynamic interactions.* The European Physical Journal E, 2005. **17**(4): p. 493-500.
229. Polin, M., et al., *Chlamydomonas Swims with Two "Gears" in a Eukaryotic Version of Run-and-Tumble Locomotion.* Science, 2009. **325**(5939): p. 487-490.
230. Gray, J.S., *Ciliary movement*. 1928: Cambridge : Cambridge university press.
231. Brumley, D.R., et al., *Flagellar synchronization through direct hydrodynamic interactions.* eLife, 2014. **3**: p. e02750.
232. Wan, K.Y. and R.E. Goldstein, *Coordinated beating of algal flagella is mediated by basal coupling.* Proceedings of the National Academy of Sciences, 2016. **113**(20): p. E2784-E2793.
233. Woolley, D.M., et al., *A study of synchronisation between the flagella of bull spermatozoa, with related observations.* Journal of Experimental Biology, 2009. **212**(14): p. 2215.
234. Gueron, S., et al., *Cilia internal mechanism and metachronal coordination as the result of hydrodynamical coupling.* Proceedings of the National Academy of Sciences, 1997. **94**(12): p. 6001-6006.
235. Guirao, B. and J.-F. Joanny, *Spontaneous Creation of Macroscopic Flow and Metachronal Waves in an Array of Cilia.* Biophysical Journal, 2007. **92**(6): p. 1900-1917.
236. Brumley, D.R., et al., *Metachronal waves in the flagellar beating of Volvox and their hydrodynamic origin.* Journal of The Royal Society Interface, 2015. **12**(108).
237. Wollin, C. and H. Stark, *Metachronal waves in a chain of rowers with hydrodynamic interactions.* The European Physical Journal E, 2011. **34**(4): p. 42.
238. Kotar, J., et al., *Optimal Hydrodynamic Synchronization of Colloidal Rotors.* Physical Review Letters, 2013. **111**(22): p. 228103.
239. Kotar, J., et al., *Hydrodynamic synchronization of colloidal oscillators.* Proceedings of the National Academy of Sciences of the United States of America, 2010. **107**(17): p. 7669-7673.
240. Koumakis, N. and R. Di Leonardo, *Stochastic Hydrodynamic Synchronization in Rotating Energy Landscapes.* Physical Review Letters, 2013. **110**(17): p. 174103.
241. O'Keeffe, K.P., H. Hong, and S.H. Strogatz, *Oscillators that sync and swarm.* Nature Communications, 2017. **8**(1): p. 1504.
242. Belovs, M., R. Livanovičs, and A. Cēbers, *Synchronized rotation in swarms of magnetotactic bacteria.* Physical Review E, 2017. **96**(4): p. 042408.
243. Snezhko, A. and I.S. Aranson, *Magnetic manipulation of self-assembled colloidal asters.* Nat Mater, 2011. **10**(9): p. 698-703.
244. Dhar, P., et al., *Active Interfacial Shear Microrheology of Aging Protein Films.* Physical Review Letters, 2010. **104**(1): p. 4.
245. Melle, S., M. Lask, and G.G. Fuller, *Pickering Emulsions with Controllable Stability.* Langmuir, 2005. **21**(6): p. 2158-2162.
246. Blanco, E., et al., *Stability and Viscoelasticity of Magneto-Pickering Foams.* Langmuir, 2013. **29**(32): p. 10019-10027.

Graphical abstract